Thermal Reactors for Emission Control

Donald J. Patterson
Department of Mechanical Engineering

and

Robert H. Kadlec
Department of Chemical Engineering

The University of Michigan

April 1971

Acknowledgement

This research was supported by the Environmental Protection Agency, the American Petroleum Institute and the Automobile Manufacturers Association, under the direction of the Coordinating Research Council.

Introduction

In recent years groups within the petroleum and automotive industries have expended considerable efforts to develop effective spark-ignition engine exhaust treatment systems. Such systems have included catalytic or non-catalytic thermal reactors or combinations of the two. Brownson (3), Chandler (6), Cantwell (4,5), Schwing (19), and Jaimee (15), have reported on the success with which non-catalytic thermal reactors oxidize the exhaust carbon monoxide and hydrocarbon constituents. These studies have provided insight into the effect that some chemical and physical factors have on reactor performance.

This paper describes progress made within the University of Michigan, Departments of Mechanical and Chemical Engineering, toward a more complete understanding of the factors governing reactor performance.

Objectives

- To quantify the effects that the various chemical and physical processes have on emission characteristics of exhaust thermal reactors installed on selected typical engines operating at various conditions on a dynamometer test stand.
- To obtain concentration measurements of pertinent chemical species and classes at the entrance to, within, and at the exit from thermal reactors, and from this data to determine gross chemical reaction rates.
- To obtain information which will be helpful in predicting the design of gasoline engine exhaust reactors.
- To develop a computer model for thermal reactors.

Part I - Thermal Reactors and Emission

The exhaust from a gasoline engine contains numerous undesirable compounds which are capable of being oxidized to carbon dioxide and water within the exhaust system. Gas chromatographic studies have revealed that exhaust gases from engines can contain two hundred or more hydrocarbon compounds, numerous aldehydes and other oxygenated and nitrated hydrocarbons. Carbon monoxide may be present to the extent of several percent. Oxides of nitrogen are additional undesirable constituents which are not capable of elimination through oxidation. The exhaust composition is strongly influenced by the fuel type and fuel-air mixture provided to the engine.

Figures 1 and 2 show a typical average dry exhaust product distribution by volume for a Chevrolet 350 $in.^3$ V-8 engine operated on an engine dynamometer at a simulated 35 mph speed (1200 rpm) at 30 horsepower. Indolene blended gasoline was used. This load simulates a moderate in-traffic acceleration maneuver of 10"-12" in. Hg. manifold vacuum. Total hydrocarbons are reported as ppm n-hexane. In addition they have been separated into classes by the technique of Sigsby (20) with the results shown in Figure 3. Aldehydes were measured by the DNPH method proposed by Oberdorfer (18) and are reported as formaldehyde in Figure 2.

Richer operation increases exhaust hydrocarbon and carbon monoxide emissions whereas nitric oxide first increases and then decreases as mixture ratio is changed. Aldehydes increase somewhat as the mixture is leaned. Hydrocarbon class percents change relatively little. At leaner mixtures the exhaust contains a higher proportion of olefins. In the absence of any exhaust treatment these constituents are emitted directly to the atmosphere.

To oxidize combustibles within the exhaust system of the engine requires adequate oxygen, temperature and residence time. It is likely that nitrogen oxides will not be eliminated or changed significantly in an oxidizing atmosphere. At best NO is converted to NO_2 within the reactor and this has no air pollution benefit. The proper combination of oxygen, temperature and residence time can be achieved by lean engine operation or air injection into the exhaust of a rich running engine, plus good exhaust energy conservation and a larger than normal insulated exhaust manifold.

Steady-State Reactor Operation

Figure 4 suggests some chemical aspects of the engine and thermal reactor. The example was developed for a rich running engine and an air injection quantity equal to 30 mole percent of the exhaust flow. Air injection fractions of .2 to .4 times exhaust flow usually yield highest conversion. In this example all the exhaust combustibles are presumed to be oxidized to CO_2 and H_2O. NO is presumed to be unaffected and shows a lower concentration exiting the reactor because of dilution. In order to adjust emission data for dilution, a correction is applied. For example, if some CO emerged from the reactor the corrected CO would be computed as:

$$(CO)_{corrected} = (CO)_{measured} \left[\frac{\text{Mole atom percent carbon without dilution}}{\text{Mole atom percent carbon with dilution}}\right]$$

All data reported herein has been corrected for dilution.

Figure 5 shows a schematic of the reactor* used with the Chevrolet 350 in^3 engine in the University of Michigan study. This was the type V reactor developed by DuPont (4). The influence of air injection fraction on the reactor performance is shown in Figure 6 for the Chevrolet engine with an air-fuel ratio of 12.5:1 operating at 1200 rpm and 30 hp. For air injection fractions between .15 and .4 good oxidation of HC and CO occurred. The exhaust gas combustibles provide the fuel energy to induce high reactor gas temperatures which in turn accelerate the reactions. Note that a 225°F gas temperature increase occurred when rapid oxidation commenced. Under rapid oxidation conditions a blue flame was apparent in the reactor. This blue flame flickered at the engine exhaust valve opening frequency. Whether or not the temperature abruptly increases and the reactions approach completion for a particular reactor input composition depends to a large degree upon the balance between energy liberated in oxidation and the extent of reaction

---

*Hereafter, the word "reactor" will include the zone between the actual reactor device and the air injection point.

determined by the reaction rate and residence time (19). Reactor temperature, heat loss, thermal inertia, and mixing are additional variables. Rapid and complete oxidation can occur with lean mixture provided heat losses are minimized.

Transient Operation

An important operating characteristic of thermal reactors is shown in Figure 7. The arrows show the direction in which the test points were run. Note that with an identical reactor input better oxidation occurred when the reactor had been hotter initially. In these tests a sufficiently long time was allowed between points to assure stabilization. This phenomena is termed "hystersis" and illustrates the importance of prior operating temperature on reactor efficiency. Thus a vehicle mounted reactor may or may not be highly efficient at a particular operating point such as idle depending on whether the engine had previously been run hard or not.

Figure 8 shows the importance of proper air injection quantity control. At too low or too high an air injection fraction of some paraffins are converted to olefins. Thus while total hydrocarbons and carbon monoxide are virtually unaffected at the operating extremes, the olefin content and therefore, exhaust reactivity has increased. Figure 9 shows the effect of air injection fraction on aldehyde emission from the reactor. Too little or too much air markedly increased aldehydes. In most air injection systems, the quantity of air is fixed at a given engine speed by the air pump which is driven off the front of the engine at a multiple of engine speed. The exhaust flow on the contrary, fluctuates widely depending on the load. Thus in practice, the operating point moves back and forth along the curves of Figures 6, 7, 8, and 9. If the air injection fraction is set at .3 for a road load condition, it can vary between .1 at WOT to .6 at idle. Obviously variations in air injection fraction depreciate optimum reactor performance.

The importance of low thermal inertia is illustrated in Figure 10. Shown is the reactor warm up from a 70°F ambient with the engine set at 1200 rpm, 30 hp and an air injection fraction of 0.3. Note that after about 5 minutes the reactor gas temperature began to increase rapidly and stabilized after 12 minutes. The reduction in NO which occurred shortly after engine start-up is thought to arise from a change in the engine and does not appear to be a repeatable characteristic. Immediately upon starting, the rapidity of the gas temperature increase depends upon mixing and expulsion of low temperature gas initially within the reactor. The mass and design of the reactor itself determine heat losses and thermal inertia and place a lower limit on the time required to light off. Figure 11 shows the engine torque, BSFC and air-fuel ratio metered to the engine for this test. Low initial torque and high BSFC result from the high friction, poor fuel distribution, and poor combustion of a cold engine. Current and future Federal emission standards for vehicles emphasize warm up.

Mixing

Temperature and composition samples measured within the thermal reactor indicate that less than perfect mixing occurs. Figure 12 compares the air-fuel ratio at three points within the reactor with the known exhaust air-fuel ratio emitted from each cylinder for cases of no air injection and two different air injection fractions. Average tailpipe air-fuel ratio is indicated also. These air-fuel ratios were calculated from the exhaust constituents by the method of Spindt (23). Note that imperfect fuel distribution within the engine itself leads to a variation in air-fuel ratio within the reactor. Cylinder No. 1 was running rich, Point A, whereas cylinders No. 3 and No. 7 were leaner, Points B and D. Note that the air-fuel ratios at this engine condition tended to be richer near the front of the engine, cylinder No. 1. The air-fuel ratios measured within the reactor, Points E, F, and G confirm that the front of the reactor was running richer than the rear. As air is injected the trend is exaggerated indicating that the rearward exhaust ports were receiving more air. The discrepancies between the average reactor internal air-fuel ratio and the average exhaust value suggest that some injected air is not mixed with the exhaust but is rapidly swept through the reactor during the blowdown pulse, mixing well enough in the remainder of the exhaust system including muffler to be measured by the continuously sampling gas instrumentation at the tailpipe. Individual measurements of hydrocarbons, CO, NO, as well as temperature, confirm the existence of a mixing problem within these reactors. Imperfect mixing causes individual elements of exhaust gas to be reacted at different average air injection fractions and temperatures. Thus the exhaust emitted from the reactor is expected to contain concentration variations which on the average means less than complete elimination of exhaust combustibles.

Conclusions

The following conclusions have been drawn regarding thermal reactor performance:

1. Exhaust gas composition, flow (reactor feed), air injection fraction, and reactor gas temperature are key parameters affecting emission reduction.
2. Under optimized conditions carbon monoxide, hydrocarbons and aldehydes can be virtually eliminated.
3. NO is largely unaffected by thermal reactors.
4. Under non-optimum air-injection conditions olefins may increase somewhat and aldehydes can increase severalfold.
5. Reactors are limited in their ability to reduce

emissions during warm-up due to low reaction rates.

6. Reactors are mixing limited under warmed up steady operation.

Part II: Simulation and Parameter Evaluation

The objective of thermal reactor design is clear: to complete the combustion of unburned and partially burned exhaust components. A number of such reactors have been built and tested, the design basis being primarily a trial-and-error procedure (5,9,10,13). The operation of non-catalytic afterburners is qualitatively simple: air and exhaust are mixed in a chamber, and oxidation proceeds, liberating heat. Carbon monoxide and hydrocarbon emissions are thereby reduced, but nitrogen oxides are not significantly altered.

The various rate processes associated with such a device can be readily identified as: heat transfer, mixing, chemical reaction and flow. The design information required thus consists of heat transfer coefficients, heat capacities, and heats of reaction; mixing parameters, reaction rate constants, and associated rate laws; and stoichiometry. Design constraints exist for the size of the reactor, the operating temperatures, the energy available for mixing, the heat losses from the reactor, and the composition, temperature and flow rate of the exhaust and added air streams.

Various attempts to explain the behavior of these reactors have met with some success. The problem encountered by all investigators is a lack of information concerning reaction rates, heat transfer and mixing. The chemical composition of the exhaust is complex and varied; therefore a class analysis of combustion rates is dictated for hydrocarbons. Paraffins, olefins, aromatics, hydrogen, and carbon monoxide form a convenient compromise between a pure component analysis and a "single-component" analysis. In general, reaction orders and rate parameters are widely variable from investigation to investigation. Heat transfer rates in odd reactor geometries can vary significantly, as can the thermal transients. Mixing is perhaps the least understood of all phenomena, and presents the worst obstacle to prediction of reactor performance.

We have not solved all of these problems, but work is proceeding to gain further data and insight concerning these interactive processes. Our goal is to divorce our approach from any specific reactor geometry - that is, to provide a general design basis which is widely applicable. Given the map of engine exhaust parameters, we wish to predict the performance of a given reactor. At this juncture, it appears that the prime design variable is the extent of mixing. Kinetics and thermal effects, on the other hand, may well be more easily predictable.

Kinetic Data

Because of the complex chemical nature of the exhaust gas, it is not feasible to incorporate a molecular kinetic mechanism in the model. There are approximately 200 identifiable hydrocarbon species present; and their oxidation probably requires many mechanistic steps, including a wide variety of free radicals in may cases. Some of the major components, such as CO and CH_4, have been investigated in some detail (2,12,14,16,17,24).

At the start of our study, the only chemical reactions considered were the oxidations of carbon monoxide and hydrocarbon as methane. Published rates for oxidation of CO are shown in Figure 13. These differ by several orders of magnitude (probably because of variations in experimental conditions). The rate equation for CO chosen for initial use in the simulation was that obtained by Yuster (24) in studies on exhaust systems.

The rate of oxidation for methane was adapted from results given by Koslov (16). Koslov's rate equation contains the partial pressure of methane raised to the -0.5 power ($P_{CH_4}^{-0.5}$); because of difficulties posed by having a rate which became infinite as concentration approached zero, this was summarily changed to $P_{CH_4}^{1.0}$ along with a compensating change in the pre-exponential coefficient to adjust the rate to match Koslov's at 600 ppm methane. The rate equations initially used were as follows:

Carbon Monoxide - Yuster

$$r_{CO} = 1.91 \times 10^2 \ e^{-35,600/RT} \ P_{CO} \ P_{O_2}$$

Methane - Koslov

$$r_{CH_4} = 2.08 \times 10^9 \ e^{-60,000/RT} \ P_{CH_4} \ P_{O_2}^{1.5}$$

Units are: r = lb moles/sec in.^{3}; T = °K; p = psia; R = 1.987 cal/g mole °K.

These rate expressions permitted early work on simulation; but the need for further data is convincingly great.

Kinetic Data - Experimental Reactor Studies

An experimental reactor was included in the program to permit a critical examination of those parameters affecting changes in the chemical composition of an elemental volume of exhaust gas as it passes through an exhaust reactor. Discussions among those involved in the study reflected the opinion that global reaction rate constants for the disappearance of certain compounds and/or classes of compounds in a perfectly mixed reactor were critical unknowns in reactor modeling. Thus the primary emphasis of the experimental reactor program has been placed on designing a system to permit the determination of these rate constants.

The stirred tank experimental reactor provides kinetic data for a perfectly mixed system. Basically this requires that air and exhaust gas of measured composition flow steadily at measured rates through a highly stirred reactor having a known and uniform pressure, temperature, and composition. Means are provided to independently vary the inlet composition, relative exhaust and air flow rates, overall flow rates, and reactor temperature.

The stirred tank system, which will also be called the two-tank system, is sketched in Figure 14. This system is attached directly to the exhaust port of a propane fueled single cylinder CFR variable compression ratio engine. Hot exhaust passes from the exhaust port through a perforated exhaust inlet tube and into a 1350 in.^{3} surge and mixing tank and then through a nozzle into the 50 in.^{3} reactor. The high velocity jets generated by the nozzle keep the reactor well stirred. Air is injected through a heated line into the reactor inlet nozzle. A throttle and by-pass loop control flowrate in order to permit the reactor residence time to be varied without changing engine conditions. The two tanks and connecting piping are constructed of Hastelloy-X and are capable of continuous operation at up to 2000°F.

Gas samples are withdrawn at the reactor inlet and outlet through water cooled sampling probes. Gas temperatures are measured with shielded thermocouples in the surge tank, at the reactor entrance, at three locations inside the reactor, and at the by-pass flowmeter. The degree of uniformity of temperature inside the reactor is checked by comparing the three thermocouple readings. As a spot check the thermocouples can be moved around inside the reactor, and in addition, the composition can be determined at various locations by inserting water-cooled sampling probes through the thermocouple taps. Surge tank and reactor pressures are measured with manometers. Propane and air flow rates to the engine as well as injection air flow rate are measured with critical flow orifices and injection air temperature with a shielded thermocouple. Flow rate through the by-pass loop is measured with a Venturi meter after the gas has been cooled by passing through a heat exchanger.

The most critical task in the reactor design was the maintenance of a high mixing rate. The mixing occurs in two steps: (1) the exhaust is mixed with air just upstream of the reactor inlet, and (2) the exhaust-air mixture is mixed with the products of reaction in the reaction chamber. In the present design both steps depend upon the mixing effects of turbulent jets. Figure 15 is a cross-section view of the reactor showing the jet orifices.

The reactor is designed to operate at a flow rate of up to 60 lbm/hr. For the present nozzle design, this requires a pressure drop of about 4 psi across the twelve 3/32 in. dia. inlet holes and results in a velocity through the holes of about 1100 ft/sec at an inlet temperature of 1000°F. The centerline velocity of a jet of this size discharging into an infinite medium would retain about 40% of its initial value after the 1.5 in. it travels in the reactor before striking a wall (see, e.g., Abramovich (1)), and thus should possess enough kinetic energy to cause a fairly high level of recirculation and turbulence in the reactor. The micro-mixing parameter of Evangelista, Shinnar, and Katz (9), which represents the ratio of residence time to micro-mixing time, is 8.5 for this system. For a given reactor volume this parameter can only be increased by decreasing the number and/or size of the inlet holes, which consequently requires a higher pressure drop across the inlet nozzle. The design permits nozzles to be easily interchanged, and the requirement of higher back pressures can be met by increasing the engine intake system pressure.

Exhaust flow rate and composition can be controlled to a large extent by individually controlling the upstream pressures of the air and fuel supplied to the engine, while temperature can be controlled by varying the engine compression ratio and spark timing. Since this does not provide much control over hydrocarbon emissions, provisions have been made to allow the introduction of species into the surge tank if this is deemed necessary. In order to permit variation of reactor residence time while holding engine conditions constant, a by-pass loop and throttle valve have been incorporated into the design. Injection air flow rate is independently controlled by adjusting the pressure upstream of the critical flow orifice, while temperature is controlled by adjusting the power to the air heaters with a variable transformer.

Helium tracer step-change tests were used to measure residence time distributions in the reactor. A photograph of a hot wire anemometer signal at the reactor exit vs. time are presented in Figure 16. For an ideal stirred tank these traces would be exponential decay curves with time constants equal to the ratio of the reactor volume V to the volume flow rate Q.

Thus the approach to stirred tank behavior can be evaluated by plotting the logarithm of the signal displacement vs. time and comparing the result to a straight line of slope -V/Q. This is done in the graphs accompanying the photographs. It is evident that the data are quite well represented by straight lines, and that the time constant τ taken from each line is in generally good agreement with the theoretical value.

The tests were run at room temperature, with the flow rates chosen to give Reynolds numbers equal to those occurring when the reactor is operating at elevated temperatures. An "equivalent flow rate", $\dot{m}_{eq}$, the mass flow rate which results in the same Reynolds number for a gas temperature of 1250°F, is noted.

A general program was written for reducing the experimental data from this test reactor on oxidation of various combustible exhaust species to a form which can be linearly regressed to obtain kinetic constants in a simplified rate correlation equation ($r = K e^{-E/RT} P_s^A P_{O_2}^B$). This program operates on flow rates for air and exhaust and concentrations entering and leaving the reactor to compute oxidative conversions. In turn, the conversions are related to the rate of reaction using the reactor design equations for an ideal back-mix reactor. Finally, logarithms are obtained for the rate r and for partial pressures P_s and P_{O_2} so that a linear regression can be performed on the log form of the rate equation.

The regression program performs an in-place inversion on the matrix of correlation coefficients using maximum pivot points. The program gives us the best values for the regression coefficients and a complete analysis of variance for the estimated value of the rate and for the contribution of each individual term within the regression equation.

Since the residence time distribution studies have indicated a behavior which is very close to an ideal stirred tank for the reactor in the two-tank system, the existing data reduction program yields at least order of magnitude results.

One hundred and ninety runs have now been completed. Inlet and outlet concentrations of CO, CO_2, H_2, NO, and hydrocarbons using both NDIR and FID analyzers, including the class breakdown by subtractive columns, were measured. The activation energy and reaction orders determined by the regression program for an assumed rate equation of the form (for CO for example):

$$r_{CO} = K \exp\left(\frac{-E}{RT}\right) P_{CO}^{A} P_{O_2}^{B}$$

were found to vary widely when data sets collected on different days under different conditions were considered separately, although a plot of the logarithm of the rate vs. 1/T reveals that at any given temperature the maximum range of measured rates is about a factor of three and the activation energy for

CO oxidation is on the order of 30,000 cal/mole. Efforts are currently being directed at finding whether inclusion of additional species in the rate equation will result in better correlation.

Thermal Effects

A program "RTEMP" has been written to simulate warm-up of an arbitrary number of metal surfaces in a reactor. Each surface, or component, exchanges heat with other surfaces or with the surroundings by radiation, subject to imposed view factors; and specified surfaces exchange heat with the exhaust gases and/or the surroundings by convection. Program parameters have initially been specified to represent the DuPont model V reactor; however, these parameters can be changed to represent almost any reactor configuration, and hence the program can be used as a design tool by making a suitable search over the design parameters.

Program "RTEMP" has been written to accept values of gas temperature from a simple kinetics simulation program. This means that operation assumes perfect mixing during warm-up, which should be acceptable during the period when conversions are definitely temperature-limited rather than mixing-limited. If necessary, "RTEMP" can be coupled with a stirred-tanks-in-series model to account for regions of different gas temperature. Such an extension would not be difficult to program, but it would likely lead to much longer running times on the computer. A summary of "RTEMP" appears in Appendix I.

The CSTR Model

A first-generation model has been developed to simulate the operation of a 300 in.^{3} reactor attached to four cylinders of a 350 in.^{3} displacement eight-cylinder engine. It is based on instantaneous mixing of air and exhaust at their repsective instantaneous flow rates at the inlet to the reactor. The reactor itself is assumed to be well stirred, meaning that temperature and composition are uniform throughout, down to the level of "micro-mixing".

Recognizing that exhaust enters in pulsations identified with the firing of individual cylinders and that the flow rate of air may be staged, the program was written to accept up to 12 input streams each of which can be timed to enter the reactor over any portion of a 720° engine cycle. The values for rate of flow, temperature, and composition for a given input are generated by function subprograms, so that any desired pattern of variation can be introduced without rewriting the calling program. Each input may contain up to 20 chemical species, which may subsequently appear as either reactants or products in any of 10 reactions.

The model computes temperatures, pressures, compositions, enthalpies, heat loss, reaction rates, outflow, and accumulation. A Runge-Kutta method of fourth order is used to compute the total moles in the reactor, the total enthalpy of the reactor, and the moles of each chemical species at any given time from rates of reaction, rates of flow, and rate of heat loss. The reactor temperature is updated for each new value of enthalpy using a half-interval root-finding technique. Pressure is computed from the total mole content of the reactor and temperature by using the perfect gas law.

Heat loss from the reactor is computed as the product of an overall heat transfer coefficeint times the difference between the temperature within the reactor and the ambient temperature. The overall coefficient has been treated as a constant and its value has been estimated, neglecting radiation, to be 0.775 Btu/°F hr, based on a reactor shell having 2 ft^2 of surface area surrounded by a 3-1/2 in. thickness of ceramic insulation. Modifications to incorporate the RTEMP calculations are also available.

Flow rate out of the reactor is computed as the product of 0.0025 times the instantaneous gage pressure within the reactor in psig. The constant 0.0025 was obtained by trial operation of the program to obtain an average operating pressure of approximately 1 psig.

Chemical reactions are communicated to the computer by arrays which give the coefficients of the chemical species in the chemical equation. Rate data for the reactions are introduced using correlations based on an Arrhenius-type power law of the form

$$r = k\, e^{-E/RT}\, P_S^A\, P_{O_2}^B$$

All of the simulations run thus far are based on selected reaction kinetics available in the literature.

A detailed description of this program is given in Appendix II.

In a typical simulation, input from each cylinder was assumed to enter at a flow, temperature, and composition which varied periodically during the course of the exhaust stroke measured in degrees of engine crank angle. The range and pattern of variation shown in Figures 17 and 18 was based on a consensus estimate by project personnel. All values shown are consistent with operation of the engine at 1200 rpm with fuel consumption of 20 lb/hr and an air/fuel ratio of 15, which is essentially the stoichiometric ratio where the fuel is assumed to be normal octane. The mass-average concentrations of combustibles entering with the exhaust were 0.8% CO and 552 ppm hydrocarbon. Additional air at 100°F was assumed to be introduced into the reactor at a constant rate, which over a cycle amounted to 40% of the entering exhaust to give a "dilution ratio" of 1.4. Exhaust temperature varied from 1200 to 2000°F.

The results of the simulation at instantaneously varying input conditions were characterized by wide swings in the outlet flow, temperature, and methane concentration and smaller variations in pressure, CO and O_2 typified by Figures 19 and 20. Performance approached repeated cyclic operation after three engine cycles of 720°, corresponding to 0.3 sec, starting with the reactor filled with nitrogen and assuming no thermal capacity in the reactor wall and insulation. Conversion of CO to CO_2 was computed to be approximately 60% and the conversion of CH_4 to CO_2 and H_2O approximately 95%. These values are in generally good agreement with experimental results given by Schwing (19) for similar operating conditions.

In a second simulation, temperature variation during the course of the exhaust stroke was averaged to give the same enthalpy input for the entering exhaust as at the instantaneous temperatures shown in Figure 17. This was accomplished by a program which determines the enthalpy of the input over one cycle of 720° from instantaneous flow, composition, and temperature, and then matches this enthalpy with a value computed from a constant temperature. The "enthalpy-averaged temperature" thus defined was computed for the instantaneous flow and composition. It should be noted that it has been shown that a summation of time-averaged composition produces the same average temperature. Since the computation was not explicit in the enthalpy-averaged temperature, the solution was obtained by using a half-interval root finding technique. Use of this enthalpy-averaged temperature in the simulation program produced conversions for CO and CH_4 that were virtually the same as for the first simulation based on instantaneous temperatures. This was true whether enthalpy-averaged temperature was used in combination with instantaneous flow and composition or with time-averaged flow and flow-averaged composition.

While our main interest is in modeling the exhaust reactor itself, the exhaust ports leading into the reactor and the exhaust pipe leaving the reactor may also provide residence times sufficient for significant amounts of reaction. To evaluate the importance of the inlet port, a stirred-tank simulation was run on a volume of 7.5 $in.^3$ receiving exhaust from a single cylinder. Inlet conditions, which averaged 0.8% CO, 552 ppm CH_4, and 1572°F, were assumed to vary periodically in the same manner as for exhaust gas entering the 300 $in.^3$ reactor. Air was introduced at 100°F to achieve a dilution ratio of 1.4 as before; however, the flow rate for the air was staged to give 10% of the average rate over the 75° interval of crank angle corresponding to maximum exhaust flow and a higher rate over the remaining 645° of a 720° engine cycle. This assumption for air rates was intended to parallel the behavior of existing methods, which tend to admit air in inverse proportion to exhaust flow because of back pressure (13).

Temperatures, pressures, and concentrations in the exhaust port were observed to exhibit periodic oscillations of wide amplitude as a function of crank angle, as would be expected for a small volume receiving a cycling input. Changes in hydrocarbon and carbon monoxide during the period after exhaust flow ceased for a cycle were represented by an exponential-type decline as combustion and dilution by the continuing flow of air dropped concentrations to near zero at the end of each 720° cycle. The most significant finding was that conversion of CH_4 was 70% and the conversion of CO 20% within the small volume of the port. It should be remembered that these conversions are based on the same selected literature values of kinetic constants used previously (24,16) and are therefore subject to an unknown error for the conditions of this problem. However, the tentative conclusion is that the exhaust port may be quite important in predicting overall conversions between the exhaust valve and the tailpipe of an exhaust system. Its importance may, however, be less than that shown due to imperfect mixing of air and exhaust within the small volume of the port.

A Micro-Mixing Model

It is characteristic of thermal exhaust reactors that small residual concentrations of carbon monoxide and hydrocarbons persist even during high-temperature operation. Depending on entering reactant concentrations and the level of turbulence, greater or lesser amounts of reaction may occur in a diffusion flame region followed by scavanging in regions which are locally homogeneous on some "macro" scale. During the composite process, small amounts of emissions escape oxidation because of inadequate mixing with air. Mixing in turn depends on the turbulent intensity and the length of time that material spends in the reactor, that is on the mean residence time and the residence time distribution.

To simulate the problem of reaction coupled with turbulent mixing, we are resorting to a random-coalescence model (RCM) that was first proposed by Curl (8). The basic assumptions of this model are that entering reactant streams can be broken down into small homogeneous cells (eddies in the case of a continuous phase) which in aggregate possess known distributions of temperature and reactant concentrations, and that mixing within the reactor can be treated in terms of random coalescences and redispersals of these cells. Reactions occur independently within each cell depending on a cell's particular temperature and composition. In the original model, the residence time distribution for cells themselves was assumed to be that for complete mixing - which implied that cells departed randomly. There is, however, no special difficulty in extending the model to any desired cell residence time distribution.

Mixing intensity in the RCM is synonymous with the coalescence frequency, which in turn can be related by means of turbulence theory to a length representing the integral scale of turbulence and a power input (or pressure drop). This relationship is derived on the assumption that mixing can be represented by stationary, isotropic turbulence (7).

The purpose in using the RCM is first to find whether mixing can be held accountable for the persistence of low levels of emissions and then to determine the extent to which performance can be improved subject to limitations on the size of a reactor and the practical level of power input for mixing represented by an allowable pressure drop.

The probability distributions for properties of cells in Curl's model can be represented by integro-differential equations, which unfortunately cannot be solved analytically (11). Some efforts have been made both currently on this project and by others to solve these equations by treating corresponding equations in the moments of the probability distributions. Without going into detail here, these efforts have not produced a method that is judged to be suitable for investigating exhaust reactors. Briefly, moment equations which are generated for integer-order chemical reactions do not represent closed sets of equations except for the trivial case of a first order reaction. For orders of 2 and higher, the effect of reaction is always represented by the highest moment, and hence there is no simple way of closing the set. Evangelista circumvented this problem by expanding the probability distribution and its moments in powers of the quotient of residence frequency over coalescence frequency, where this quotient goes to zero for complete mixing. This method, however, is restricted to rate expressions which can be expressed as polynomials in concentration and to steady state solutions. In view of this complexity (which masks the salient features of the model), it is not felt to be applicable to our problem.

The alternatives to treating moment equations is to treat the integro-differential equations numerically or to apply Monte Carlo methods directly to the model itself (22). The latter is a highly flexible approach which preserves close at hand the basic assumptions in the model. It is therefore the approach which is being used in further work on mixing.

A first version of a computer program, "MICRO MIX I", based on the random coalescence model has been completed. This first version assumes that cells are themselves perfectly mixed and therefore leave the reactor randomly. It is planned that future versions of the program will be developed to treat the cases of axially segregated flow and of an assigned residence time distribution.

Input to MICRO MIX I consists of a periodic sequence of cells which follows as closely as is known the actual inputs from cylinders and air jets. Thus the temperature and composition of cells varies periodically over a period corresponding to 720° of engine revolution; and cells of air and exhaust are interspersed in the input according to their varying ratio of flow during that cycle.

Within the reactor, cells are chosen randomly to coalescence with each other and to collide with the reactor wall. The rate of coalescence is computed from a characteristic length, the pressure drop, and gas flow. The frequency of wall collision is computed to satisfy the overall heat loss corresponding to a specified heat transfer coefficient based on the assumption that cells striking the wall assume the wall temperature.

Cell temperature and composition are updated prior to coalescence, wall collision, or departure from the reactor. The updating procedure is based on equations for adiabatic batch reaction. Integrations are performed using a simple midpoint slope method and a step size which is computed to involve no more than 10% depletion of any remaining species. This highly simplified method of integration was chosen to provide rapid computation, which is considered necessary to compensate for the time-penalty of following large numbers of cells. Although the method does not possess a high precision, small inaccuracies in the integration of the homogeneous kinetics will not prevent the program from reaching a valid mean conversion were the latter is primarily controlled by mixing.

During operation of the program, the distribution of concentrations and temperatures in the cells within the reactor converge from a specified initial distribution to a quasi-steady-state distribution which is the result of the coupled effects due to inputs, coalescence frequency, wall collision frequency, residence frequency, and reaction. The progress of convergence is followed by determining the mean properties and the variance (second moment about the mean) for successive sets of "NCC" cells leaving the reactor, where "NCC" is the number of cells that are introduced in one engine cycle.

A summary of this program appears in Appendix III.

Conclusions

The following conclusions can be drawn regarding thermal reactor simulation:

1. The key parameters in a simulation are feed composition, temperature and flow; reaction, heat transfer and mixing rates; and the residence time distribution.

2. Warm-up computations, in general, differ from computations of steady operation.

3. It is impractical to consider all individual chemical species.

4. It is impractical to deal with mechanistic rate laws.

5. Reactor materials (their heat capacity and thermal conductivity) to a large extent determine warm-up time.

Appendix I

FLOW SHEET FOR SUBROUTINE "RTEMP"

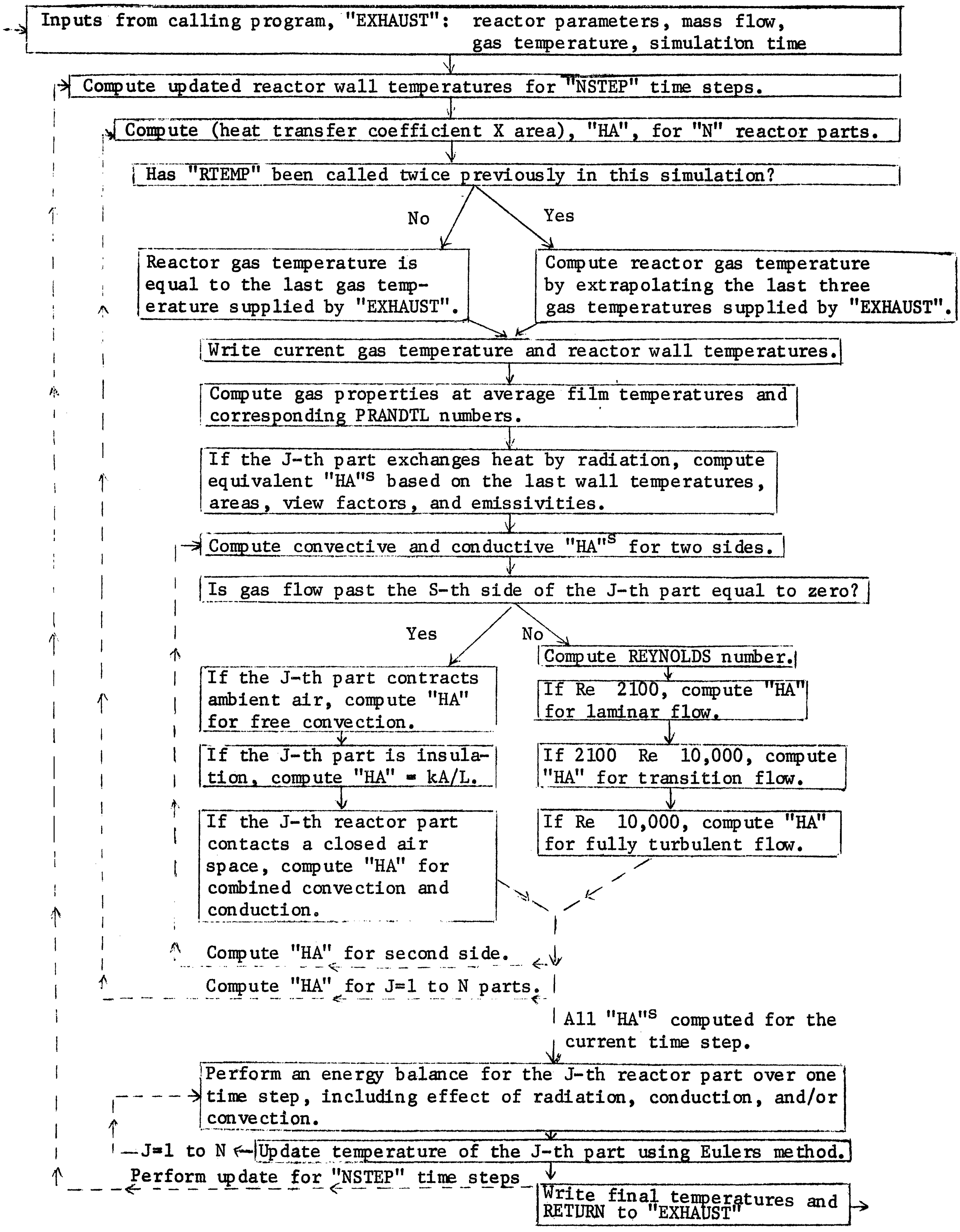

Appendix II

FLOW DIAGRAM OF PROGRAM OPERATION - PROGRAM EXHAUST

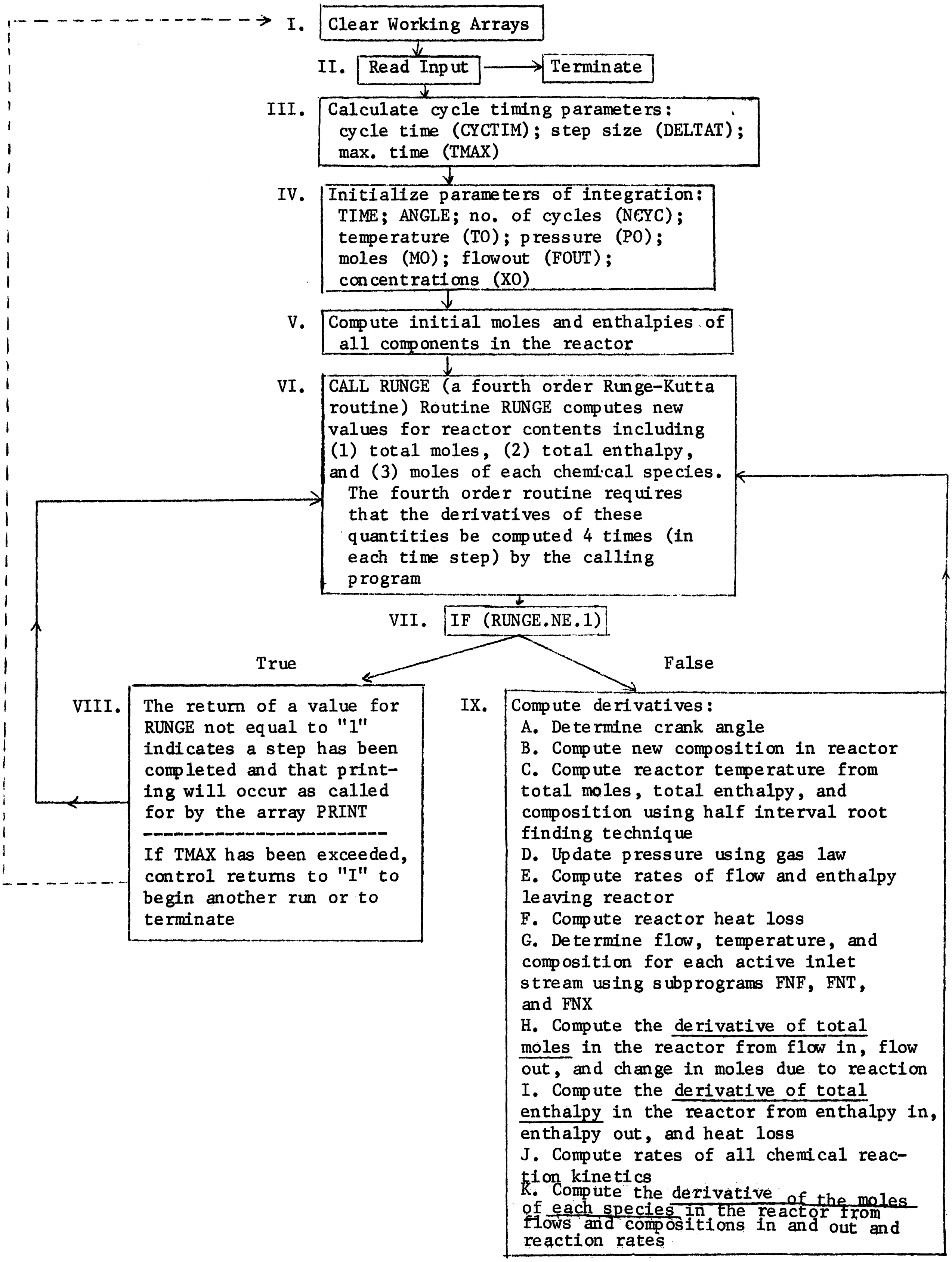

I. Clear Working Arrays

II. Read Input

III. Calculate cycle timing parameters: cycle time (CYCTIM); step size (DELTAT); max. time (TMAX)

IV. Initialize parameters of integration: TIME; ANGLE; no. of cycles (NCYC); temperature (TO); pressure (PO); moles (MO); flowout (FOUT); concentrations (XO)

V. Compute initial moles and enthalpies of all components in the reactor

VI. CALL RUNGE (a fourth order Runge-Kutta routine) Routine RUNGE computes new values for reactor contents including (1) total moles, (2) total enthalpy, and (3) moles of each chemical species. The fourth order routine requires that the derivatives of these quantities be computed 4 times (in each time step) by the calling program

VII. IF (RUNGE.NE.1)

VIII. The return of a value for RUNGE not equal to "1" indicates a step has been completed and that printing will occur as called for by the array PRINT

If TMAX has been exceeded, control returns to "I" to begin another run or to terminate

IX. Compute derivatives:

A. Determine crank angle

B. Compute new composition in reactor

C. Compute reactor temperature from total moles, total enthalpy, and composition using half interval root finding technique

D. Update pressure using gas law

E. Compute rates of flow and enthalpy leaving reactor

F. Compute reactor heat loss

G. Determine flow, temperature, and composition for each active inlet stream using subprograms FNF, FNT, and FNX

H. Compute the derivative of total moles in the reactor from flow in, flow out, and change in moles due to reaction

I. Compute the derivative of total enthalpy in the reactor from enthalpy in, enthalpy out, and heat loss

J. Compute rates of all chemical reaction kinetics

K. Compute the derivative of the moles of each species in the reactor from flows and compositions in and out and reaction rates

Appendix II-2

LIST OF DATA INPUTS

Specific heat constants	(A,B,C,D)
Heats of formation	(DHF)
Molecular weights	(MWT)
Gas constants	(RG & RK)
Number of inputs	(N)
Number of chemical species	(M)
Number of reactions	(Q)
Pre-exponential rate coefficients	(AA)
Activation energies	(E)
Stoichiometric coefficients	(NU)
Reaction rate exponents (orders)	(NE)
Engine rpm	(LAMBDA)
Input crank angles	(ALOW)
Crank angle spans for inputs	(ASPAN)
Minimum temperatures of inputs	(TLOW)
Temperature spans of inputs	(TSPAN)
Minimum flow rates of inputs	(FLOW)
Flow spans of inputs	(FSPAN)
Minimum concentrations in inputs	(XLOW)
Concentration spans of inputs	(XSFAN)
Reactor volume	(V)
Ambient pressure	(PA)
Ambient temperature	(TA)
Heat transfer coefficient (overall)	(HRAR)
Flow coefficient	(CFLOW)
Initial reactor temperature	(TOZERO)
Initial reactor pressure	(POZERO)
Initial reactor compositions	(XOZERO)
Tolerance for temperature calculations	(TEPS)
Duration of simulation in engine cycles	(MAXCYC)
Number of computational steps per cycle	(NSPCYC)
Print frequency	(FREQ)
Maximum number of half-interval iterations	(ITMAX)
Print control	(PRINT)

MAXIMUM NUMBER OF PRINTED OUTPUTS

Numbers of inputs, species, and reactions
Heats of formation and specific heats
Stoichiometric equations and chemical rate equations
input parameters
    engine rpm
    input timing
    temperature
    flow
    composition
Initial and ambient conditions
computational and printing parameters
Reactor temperature, pressure, and mole balance versus crank angle
Reactor composition versus crank angle
Inlet flow, temperature, and enthalpy versus crank angle
Inlet composition versus crank angle
Energy balance versus crank angle
Reaction rates versus crank angle
Rates of species "appearance" versus crank angle
Intermediate computations used for debugging

NOTES:

1. Subprograms FNF, FNT, and FNX supply values of flow, temperature, and composition as functions of crank angle.
2. All enthalpies are generated by a subroutine HMOLAR based on temperatures, specific heats, and heats of formation supplied by the calling program.
3. All time advance is accomplished within subprogram RUNGE.

FLOWSHEET FOR REACTOR MIXING SIMULATION, "MICRO MIX I"

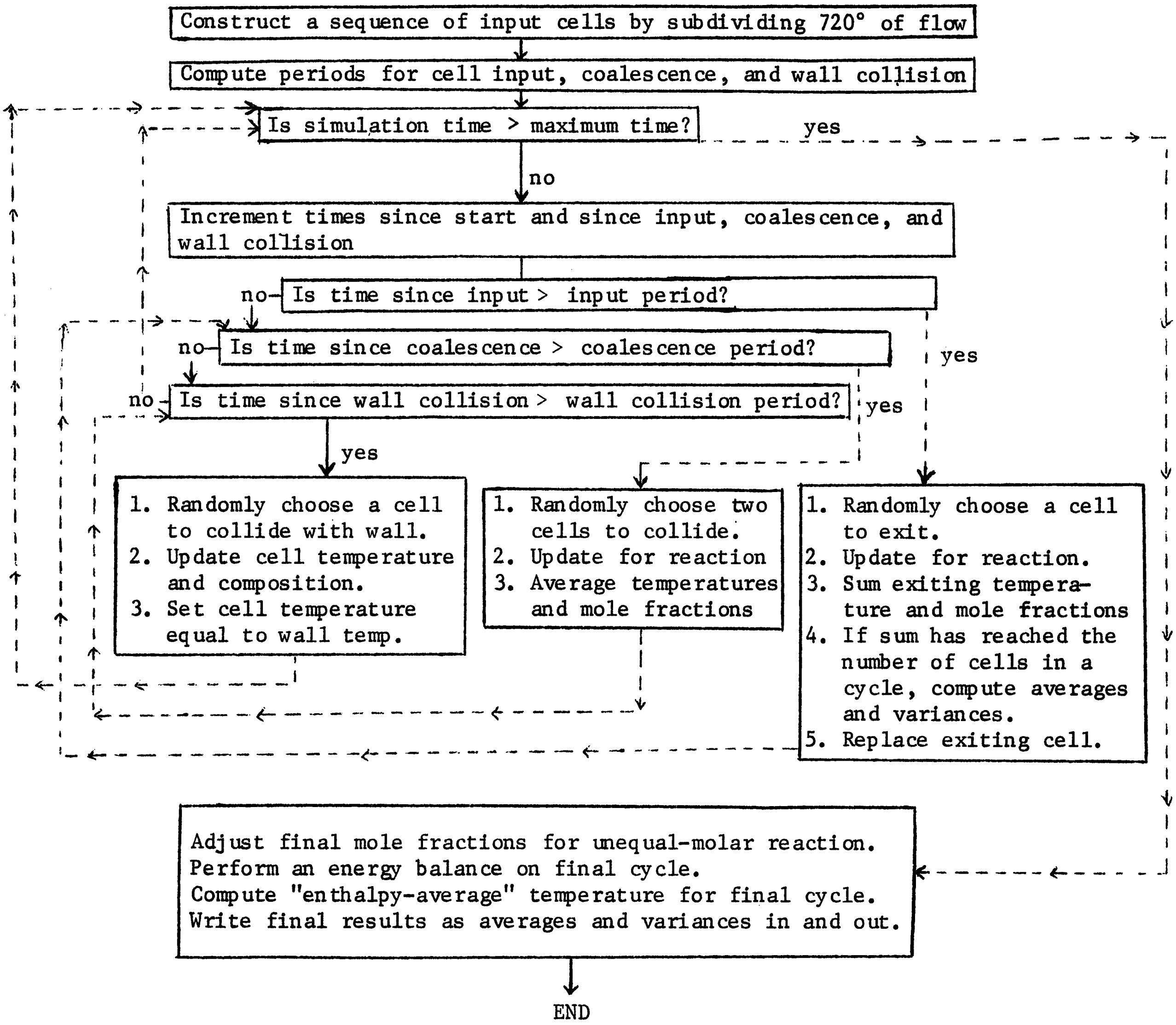

COUPLING OF MAIN PROGRAM "EXHAUST" WITH WARMUP SUBROUTINE "RTEMP"

Program "EXHAUST" computes emission conversions and reactor gas temperature based on the design equations for a well stirred reactor. The version which is coupled to "RTEMP" accepts only steady input flow with uniform properties. The heat exchange between reactor gas and reactor walls in the heat balance is computed separately for as many reactor parts as have a different temperature and contact the exhaust gas.

The flow sheet for "EXHAUST" that follows describes only those actions which specifically relate to subroutine "RTEMP".

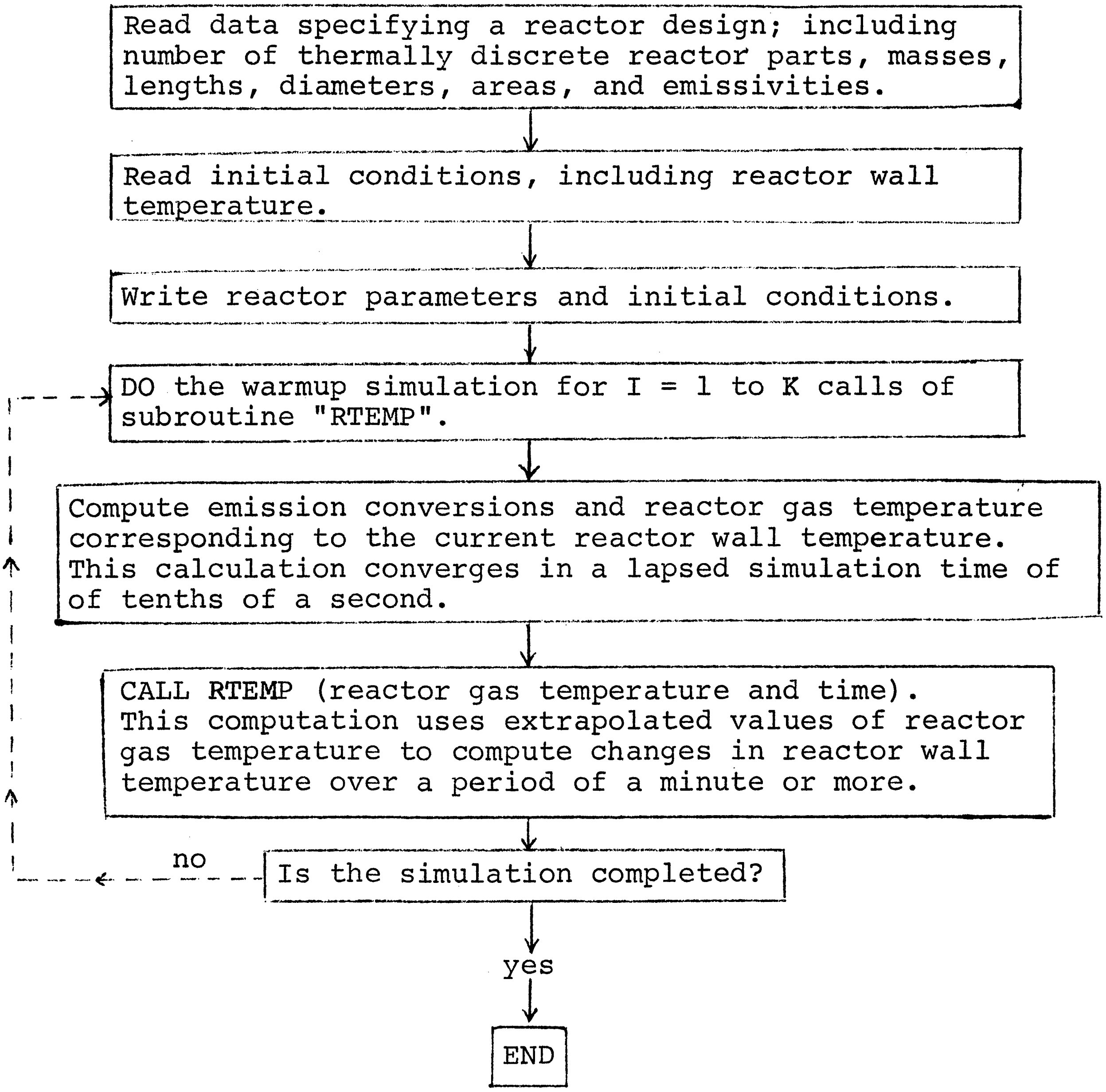

References

1. Abramovich, The Theory of Turbulent Jets, M.I.T. Press (1963).

2. Baum, E., "Automobile Afterburner Studies: Noncatalytic Afterburning Without Ignition", U.C.L.A. Report 59-14, March 1959.

3. Brownson, D. A., and R. F. Stebar (General Motors), "Factors Influencing the Effectiveness of Air Injection in Reducing Exhaust Emissions", Society of Automotive Engineers, TP-12, p. 103. (Originally published in SAE Transactions, 74, 1966.)

4. Cantwell, E. N., I. T. Rosenlund, W. J. Barth, F. L. Kinnear, and S. W. Ross (DuPont), "A Progress Report on the Development of Exhaust Manifold Reactors", Paper No. 69-139, SAE International Automotive Engineering Congress, Detroit, Michigan, January 13-17, 1969.

5. Cantwell, E. N., and A. J. Pahnke (DuPont), "Design Factors Affecting the Performance of Exhaust Manifold Reactors", SAE Transactions, 74, 1966.

6. Chandler, J. M., A. M. Smith, and J. H. Struck (Ford), "Development of the Concept of Non-flame Exhaust Gas Reactors", Paper No. 486M, SAE National Automobile Week, March 1962.

7. Corrsin, S., "The Isotropic Turbulent Mixer: Part II. Arbitrary Schmidt Number", A.I.Ch.E. Jour., 10 870(1964).

8. Curl, R. L., "Dispersed Phase Mixing: I. Theory and Effects in Simple Reactors", A.I.Ch.E. Jour., 9, 175 (1963).

9. Evangelista, J. J., R. Shinnar, and S. Katz, "The Effect of Imperfect Mixing on Stirred Combustion Reactors", 12th Symposium (Int'l) on Combustion, pp. 901-912 (1969).

10. Evangelista, J. J., R. Shinnar, and S. Katz, "The Effect of Incomplete Mixing in Stirred Combustion Reactors", Twelfth Symposium (International) on Combustion, Poitiers, France, July 1968.

11. Evangelista, J. J., R. Shinnar, and S. Katz, "Scale-Up Criteria for Stirred Tank Reactors", A.I.Ch.E. Jour., 15, 6, 843 (1969).

12. Fristrom, R. M., and A. A. Westenberg, Flame Structure, McGraw-Hill, New York, 1965, p. 349.

13. Glass, W., D. S. Kim, and B. J. Kraus (Esso), "Synchrothermal Reactor System for Control of Automotive Exhaust Emissions", SAE Paper No. 700147, Automotive Engineering Congress, Detroit, Michigan, January 12-14, 1970.

14. Hottel, H. C., G. C. Williams, N. M. Nerheim, and G. R. Schneider, "Kinetics Studies in Stirred Reactors: Combustion of Carbon Monoxide and Propane", Tenth Symposium (International) on Combustion, 1965, p. 111.

15. Jaimee, A., et al., "Thermal Reactors - Design, Development and Performance", SAE Preprint 710293, January 1971.

16. Koslov, G. I., "On High Temperature Oxidation of Methane", Seventh Symposium (International) on Combustion, 1958, p. 142.

17. Longwell, J. P., and M. A. Weiss (Esso), "High Temperature Reaction Rates in Hydrocarbon Combustion", Industrial and Engineering Chemistry, 47, No. 8, 1634 (August 1955).

18. Oberdorfer, P. E., "Determination of Aldehydes in Automotive Exhaust Gas", SAE Preprint 670123, January 1967.

19. Schwing, R. C. (General Motors), "An Analytical Framework for the Study of Exhaust Manifold Reactor Oxidation", SAE Preprint 700109, January 1970.

20. Sigsby, J. E., Jr. and D. L. Klosterman, "Application of Subtractive Techniques to the Analysis of Automotive Exhaust", Environmental Science & Technology, vol. 1, no. 4, April 1967, p. 311.

21. Sorenson, S. C., P. S. Myers, O. A. Uyehara, "The Reactions of Ethane in Spark-Ignition Engine Exhaust Gas", SAE Preprint 700471, May 1970.

22. Spielman, L. A., and O. Levenspiel, "A Monte Carlo Treatment for Reacting and Coalescing Dispersed Phase Systems", Chem. Eng. Science, 20, 247 (1965).

23. Spindt, R. S., "Air-Fuel Ratios from Exhaust Gas Analysis", SAE Transactions, vol. 74, 1966.

24. Yuster, S. T., Stoudhammer, J. Miller, S. Sourirajan, R. Henderson, and T. Masters, "Afterburner Studies as Applied to Automobile Exhaust Systems", U.C.L.A. Report 58-55, June 1958.

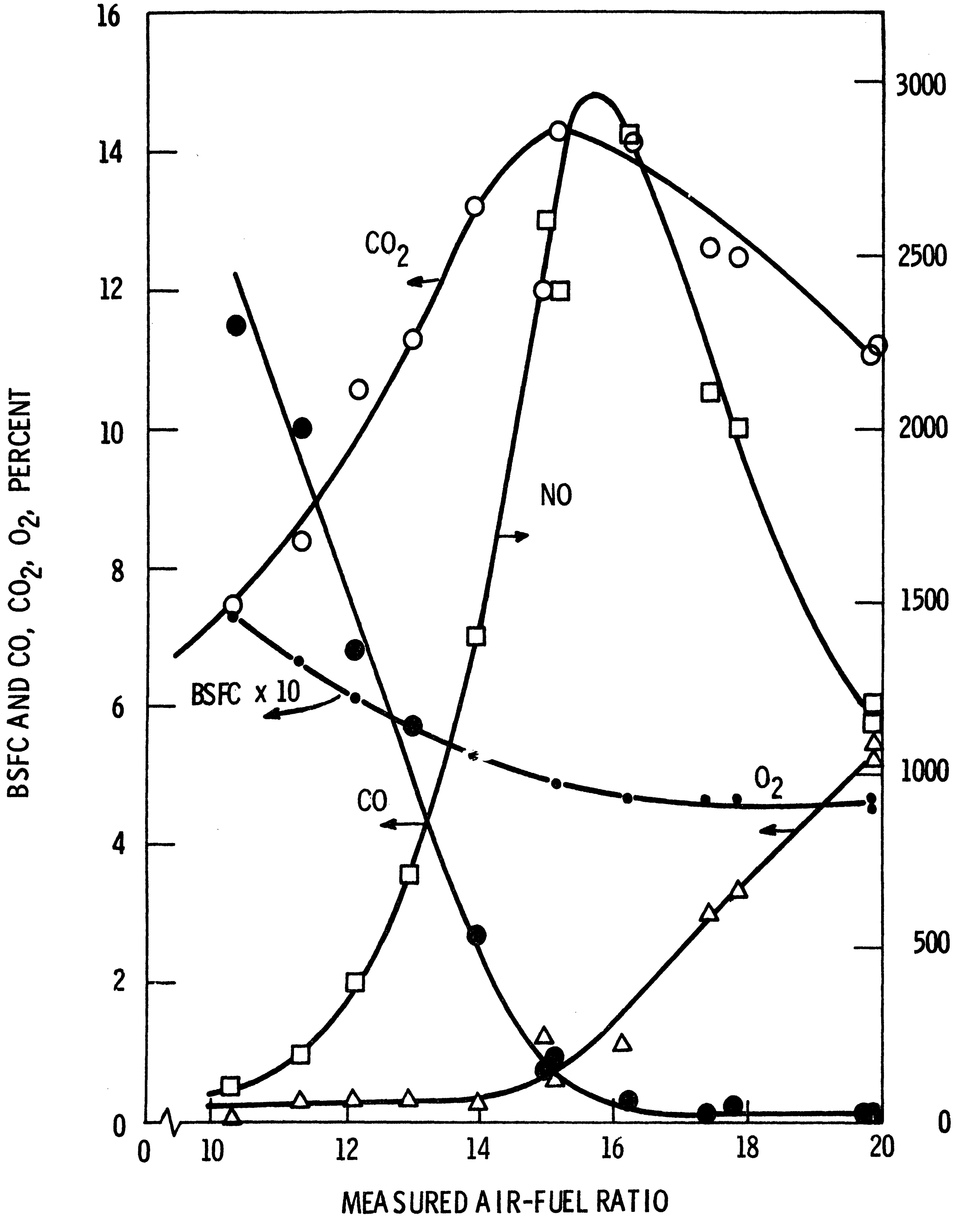

Figure 1. CO_2, CO, O_2, and NO emission vs. air-fuel ratio. 1200 rpm, 50% load, MBT spark, Indolene clear fuel.

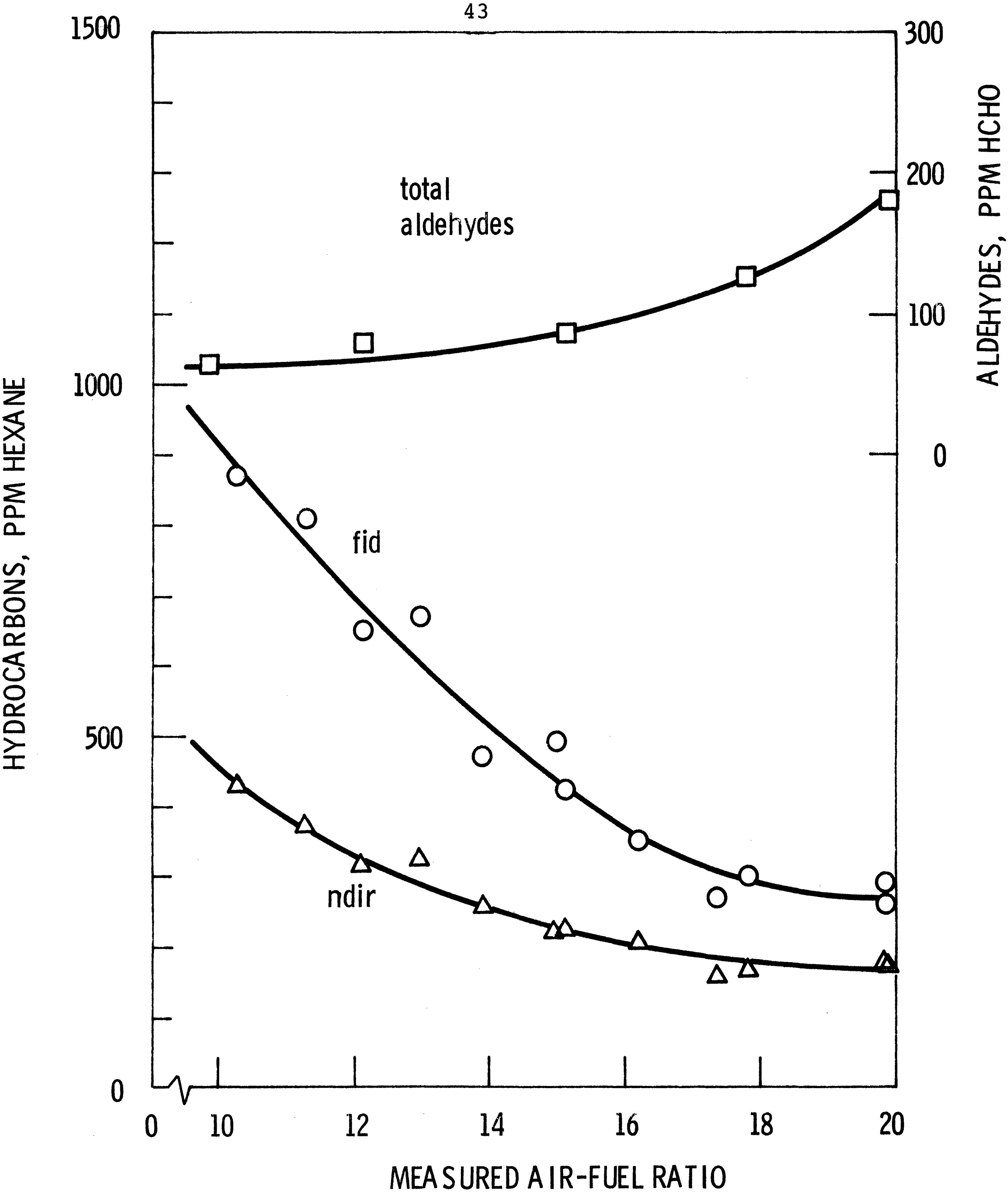

Figure 2. Hydrocarbon and aldehyde emission vs. air-fuel ratio. Engine conditions of Figure 1.

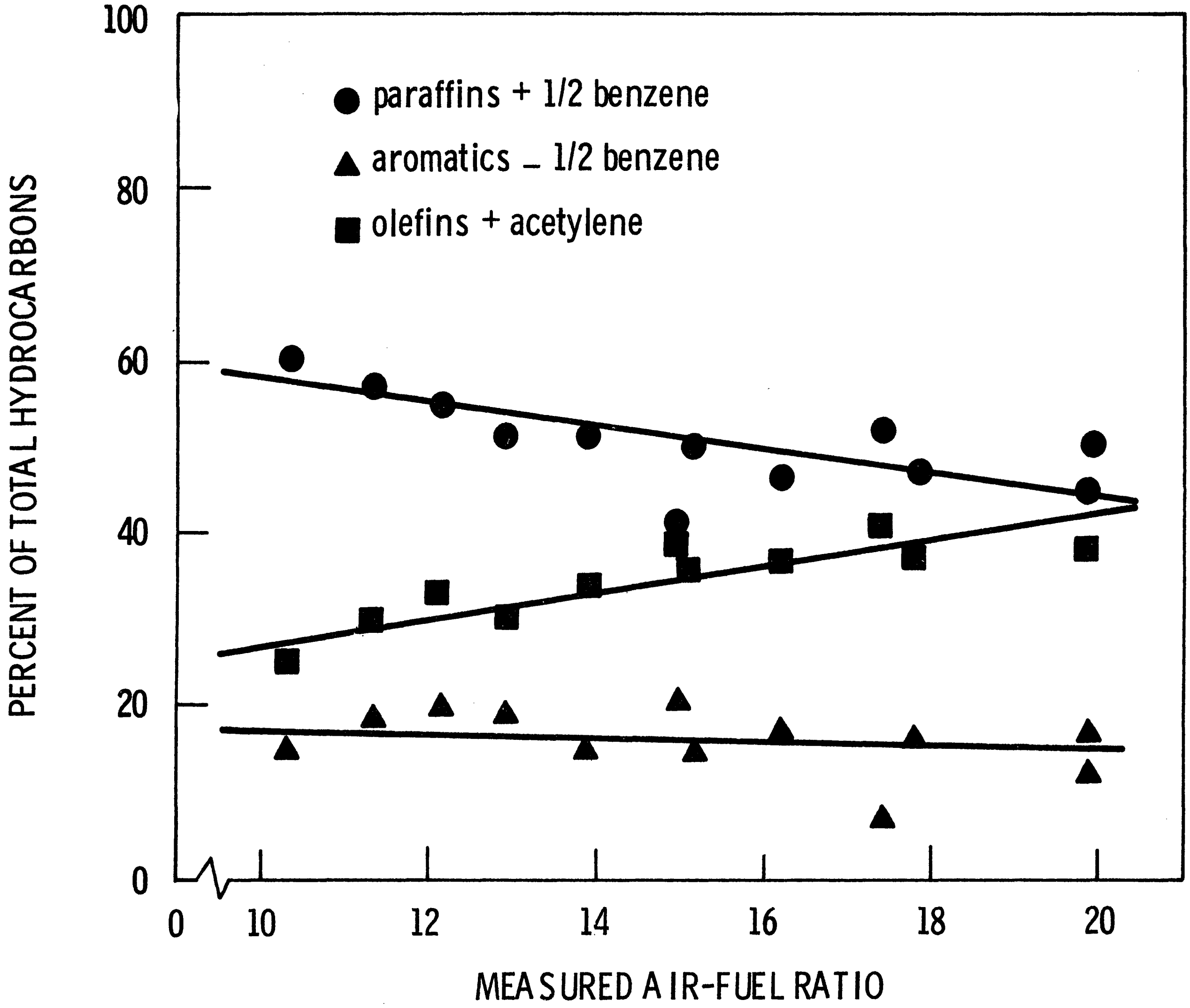

Figure 3. Hydrocarbon class analysis vs. air-fuel ratio. Engine conditions of Figure 1.

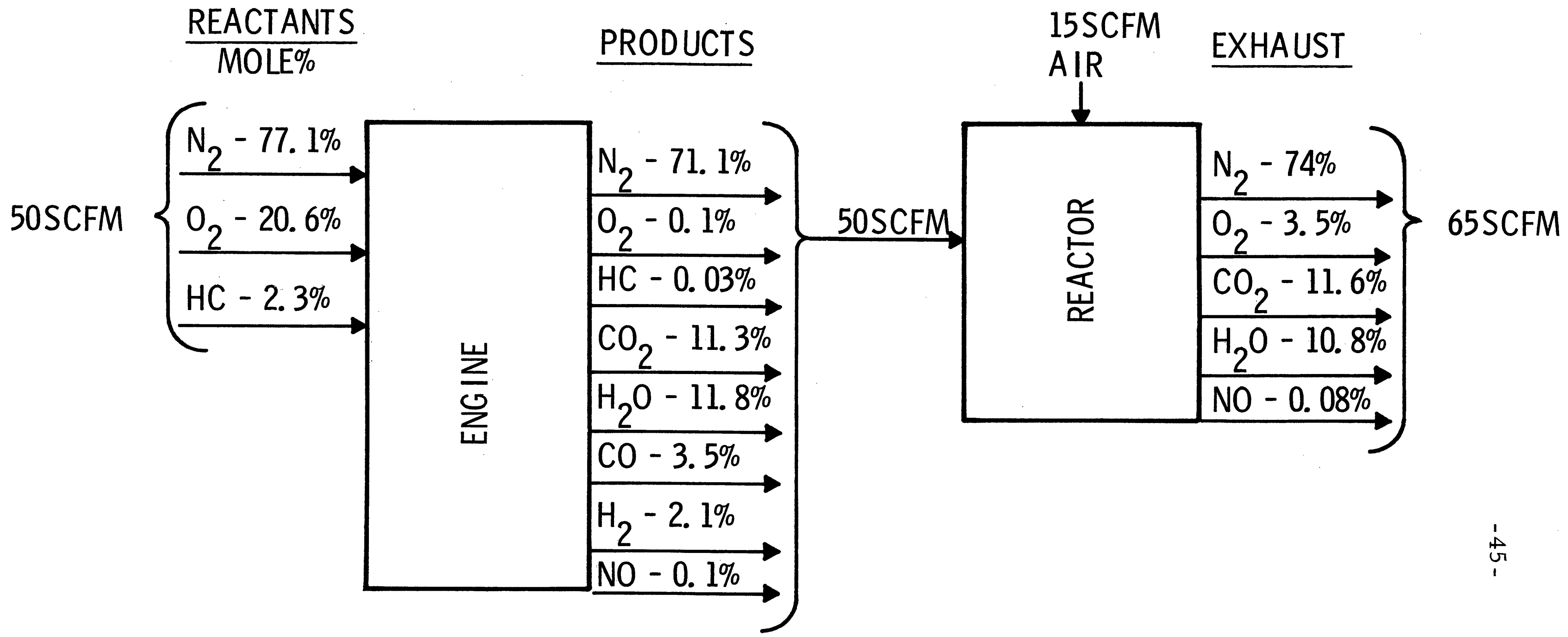

Figure 4. Engine-reactor stoichiometry.

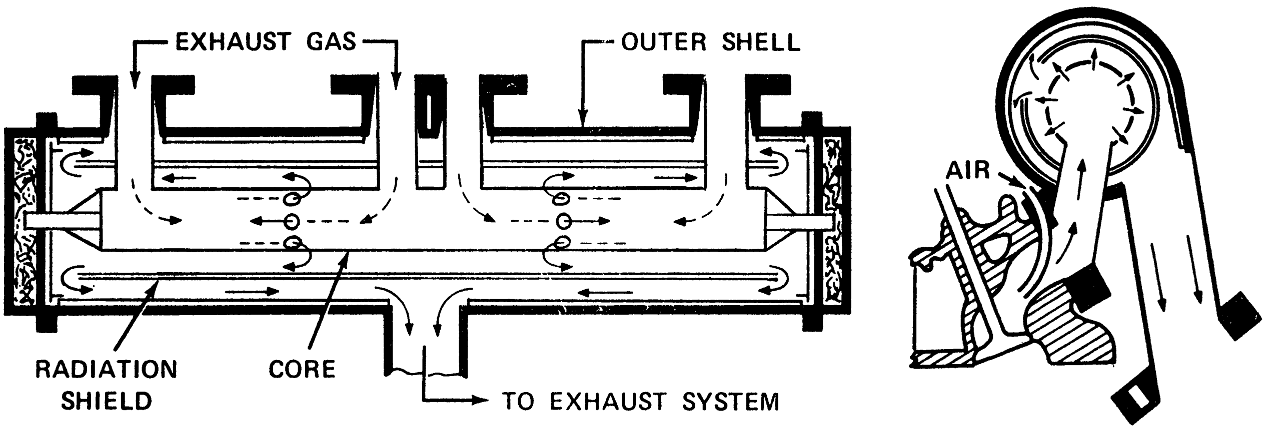

Figure 5. Type V DuPont exhaust manifold reactor. Figure courtesy DuPont Corporation.

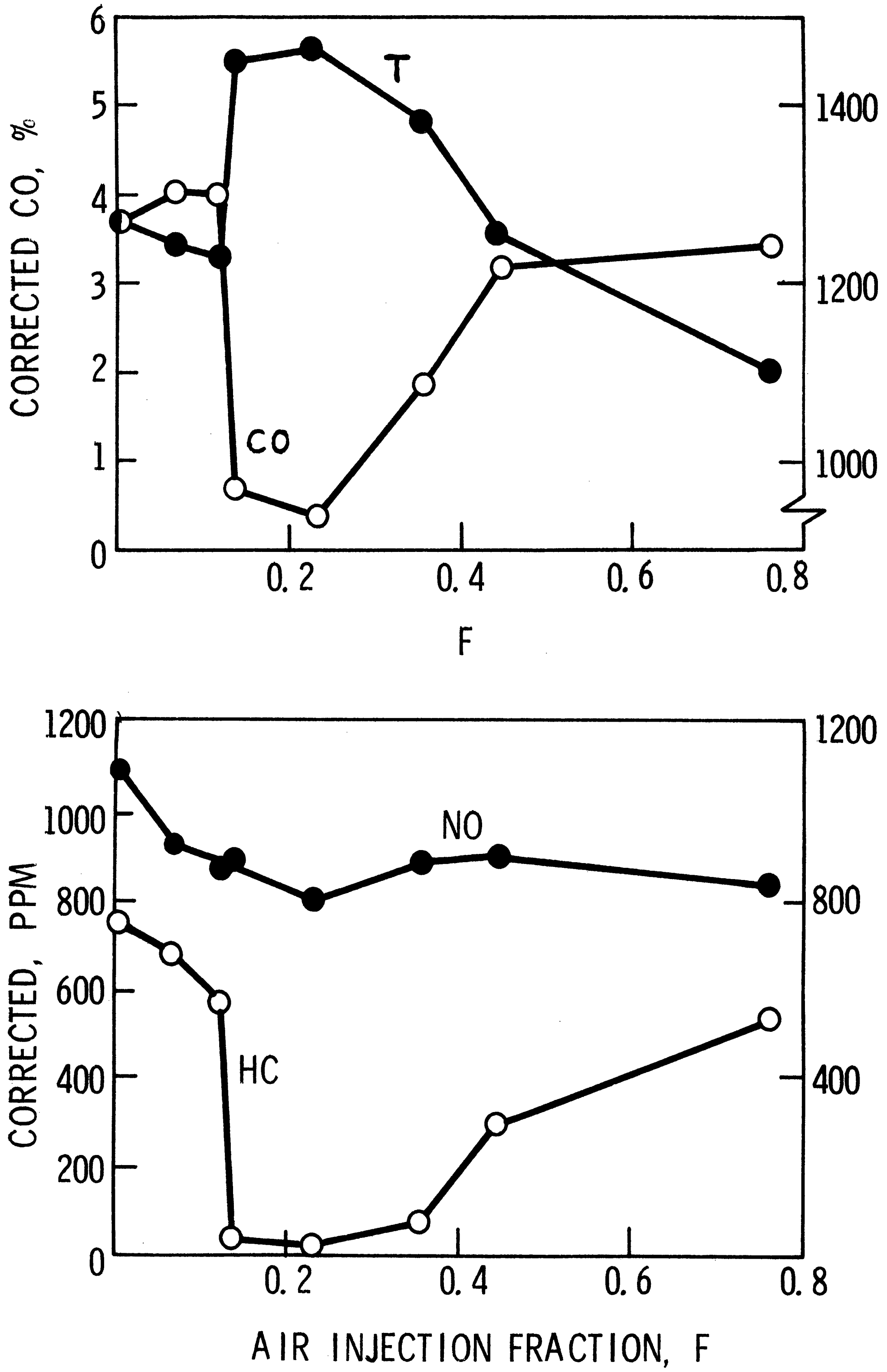

Figure 6. Exhaust emissions and reactor gas temperature as a function of air injection fraction. 1200 rpm, 50% load, 12.7:1 air-fuel ratio, MBT spark.

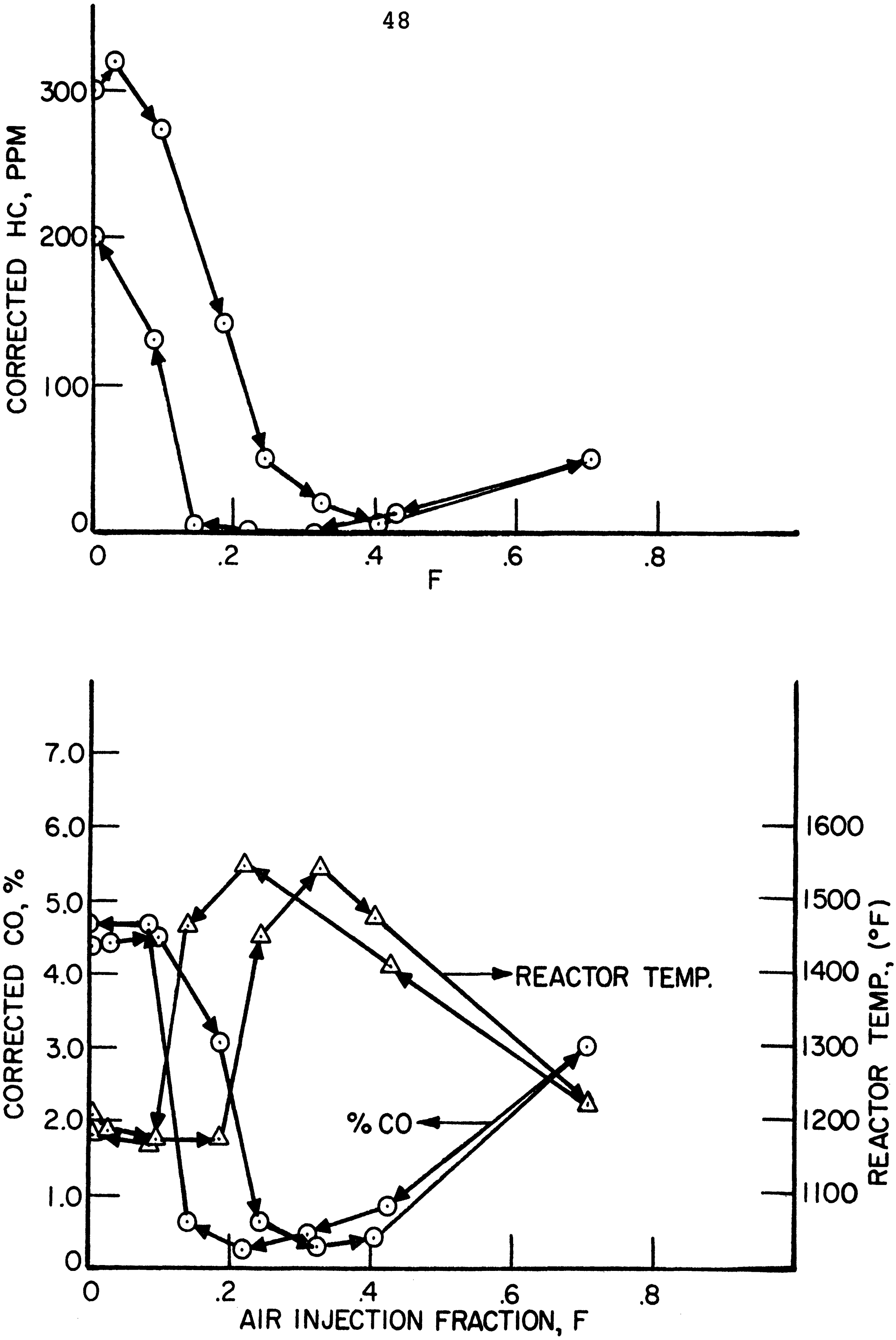

Figure 7. Exhaust emissions and reactor temperature as a function of air injection fraction. 12.3:1 air-fuel ratio. Arrows indicate direction in which test was run. The non-repeatibility is termed hysteresis.

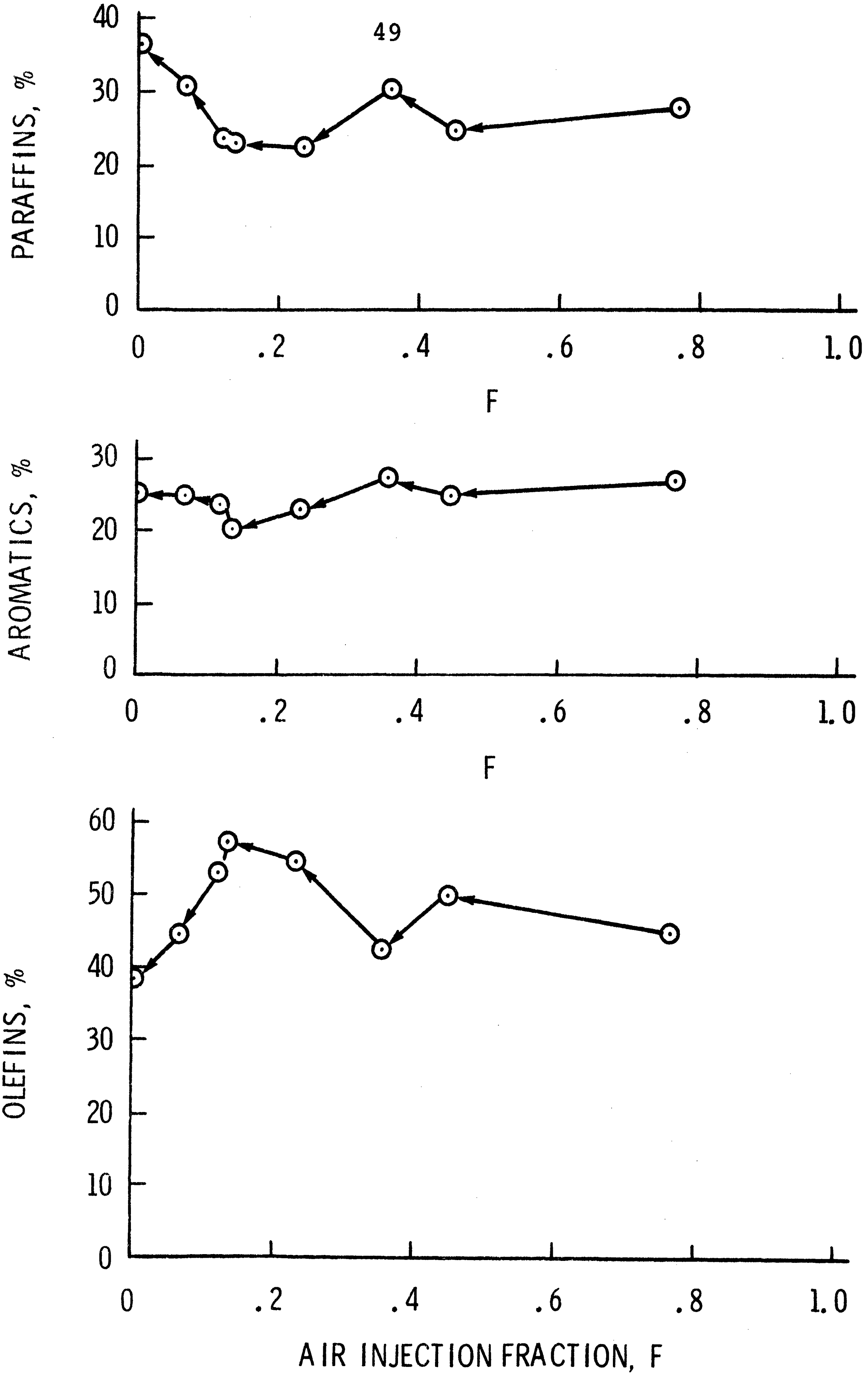

Figure 8. Class analysis percent versus air injection fraction at 12.5:1 air-fuel ratio. Engine conditions of Figure 6.

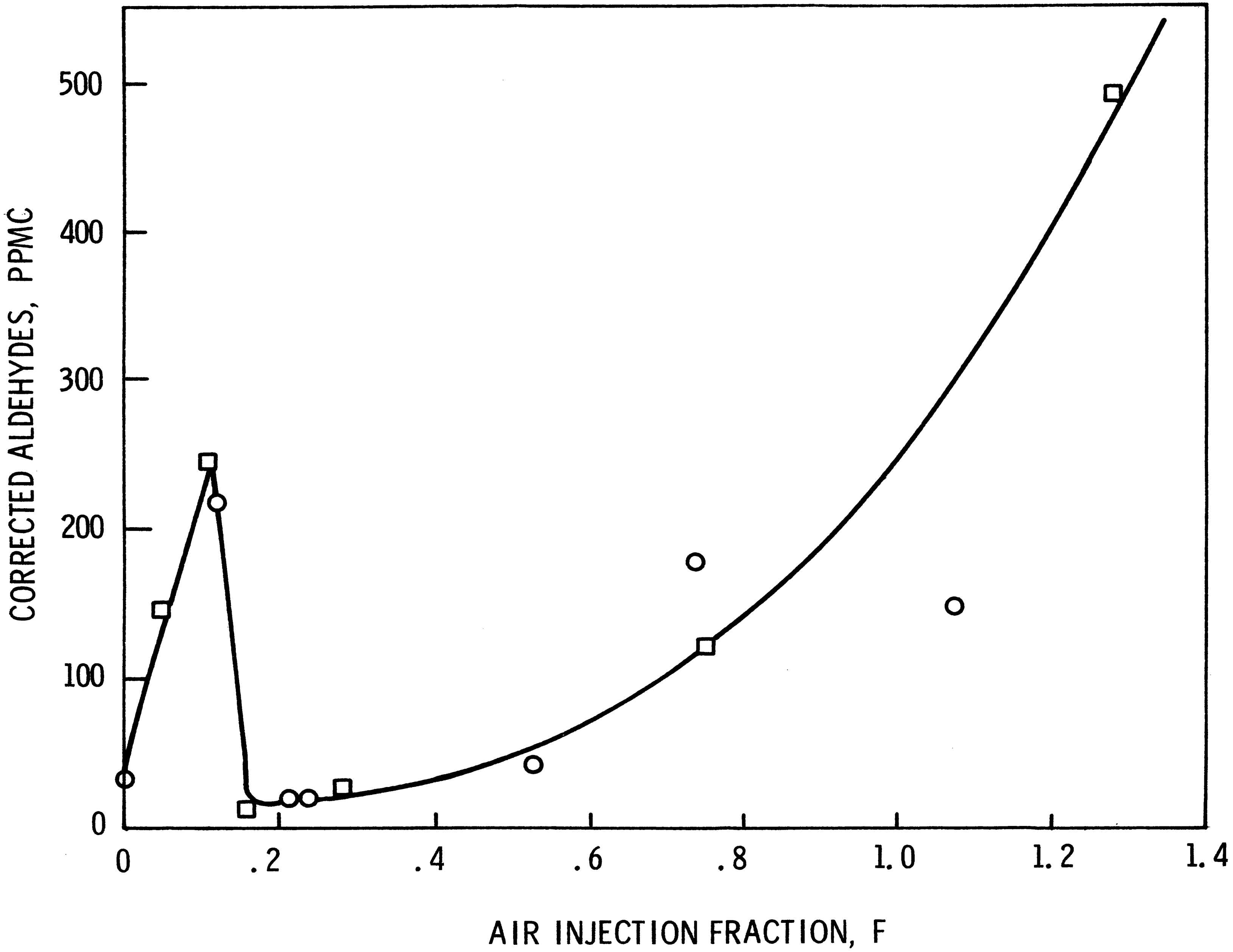

Figure 9. Aldehyde emission vs. air injection fraction. Engine conditions of Figure 6. Data measured on two days.

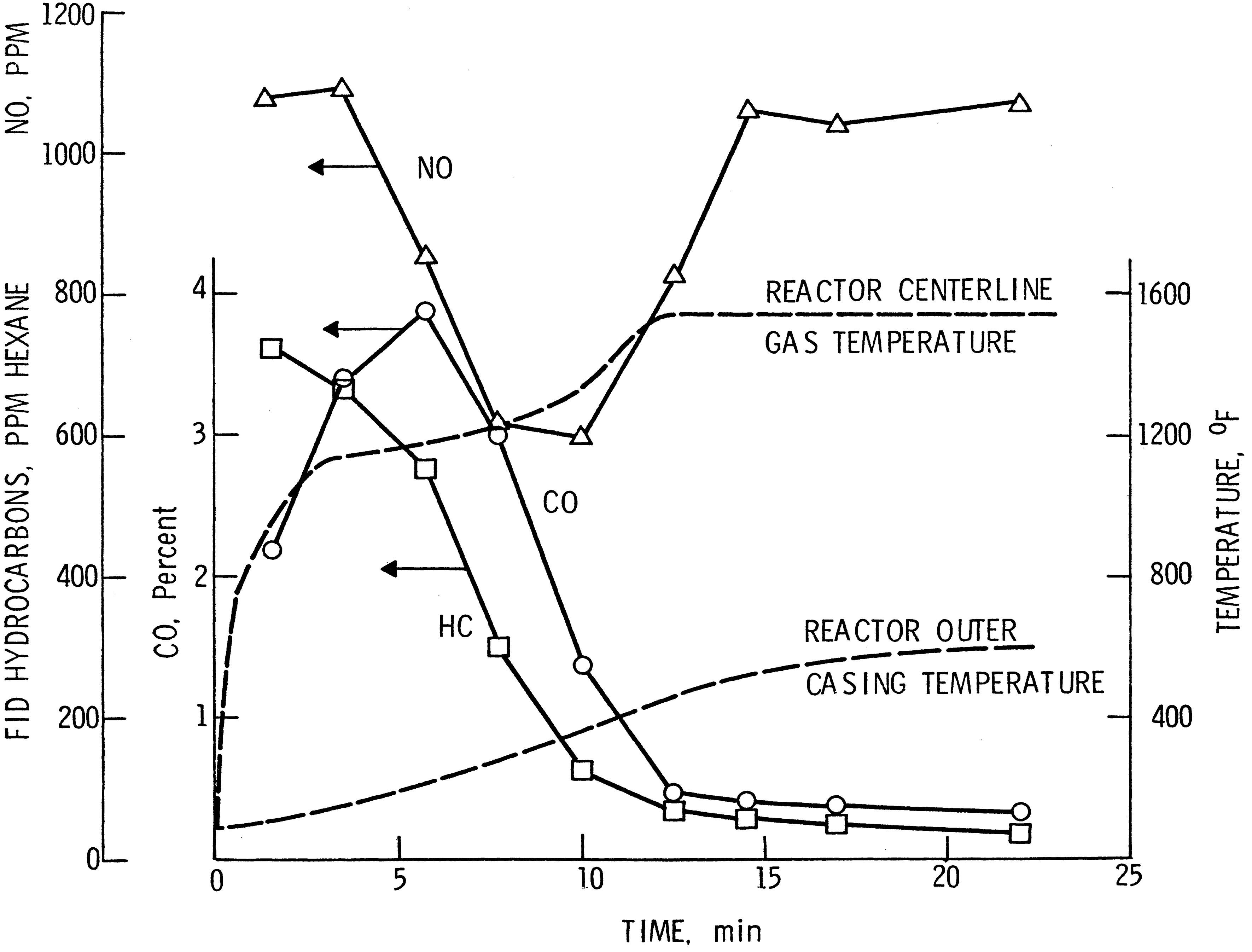

Figure 10. Thermal reactor warm-up.

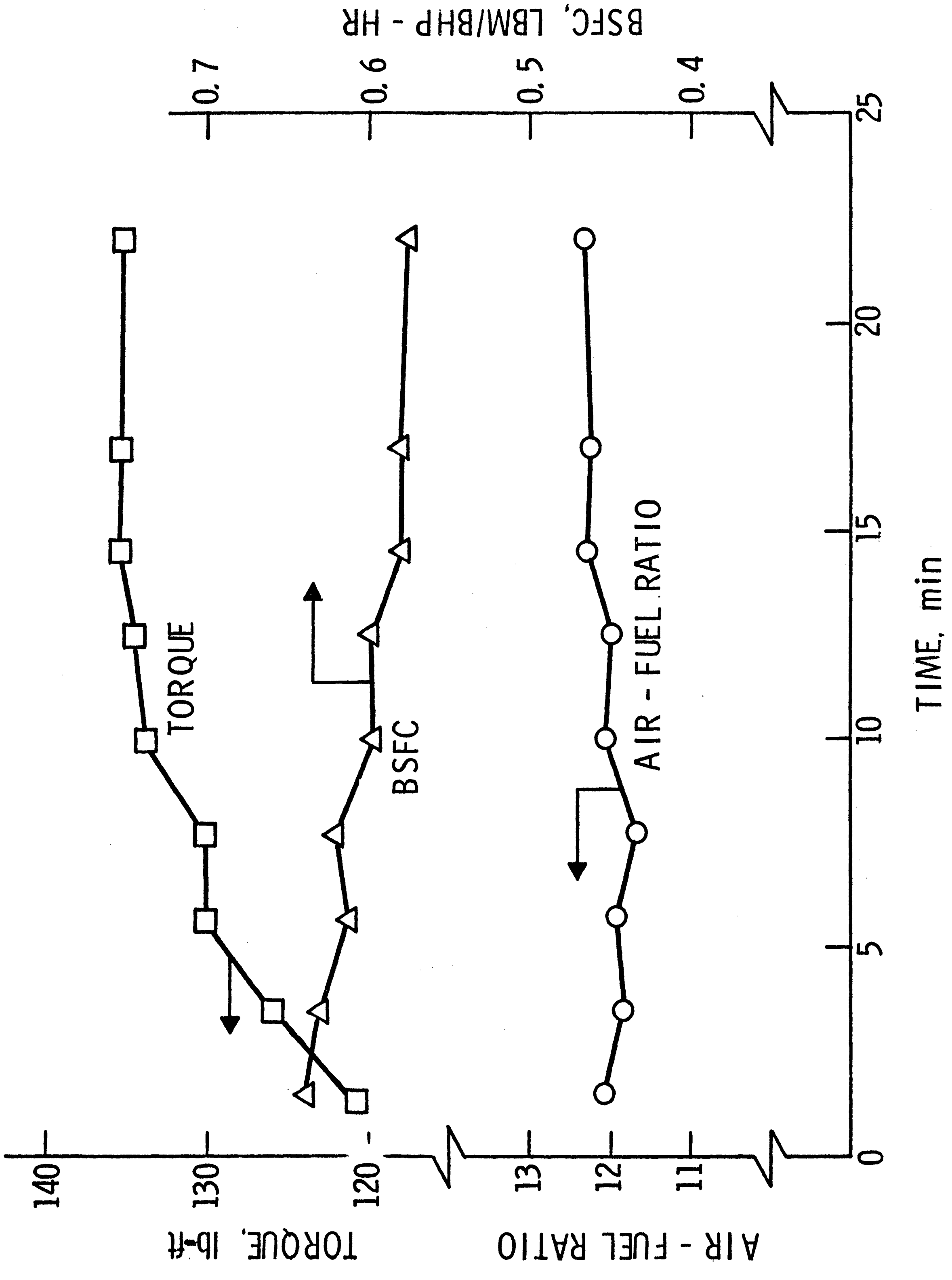

Figure 11. Engine parameters during warm-up (corresponds to Figure 10).

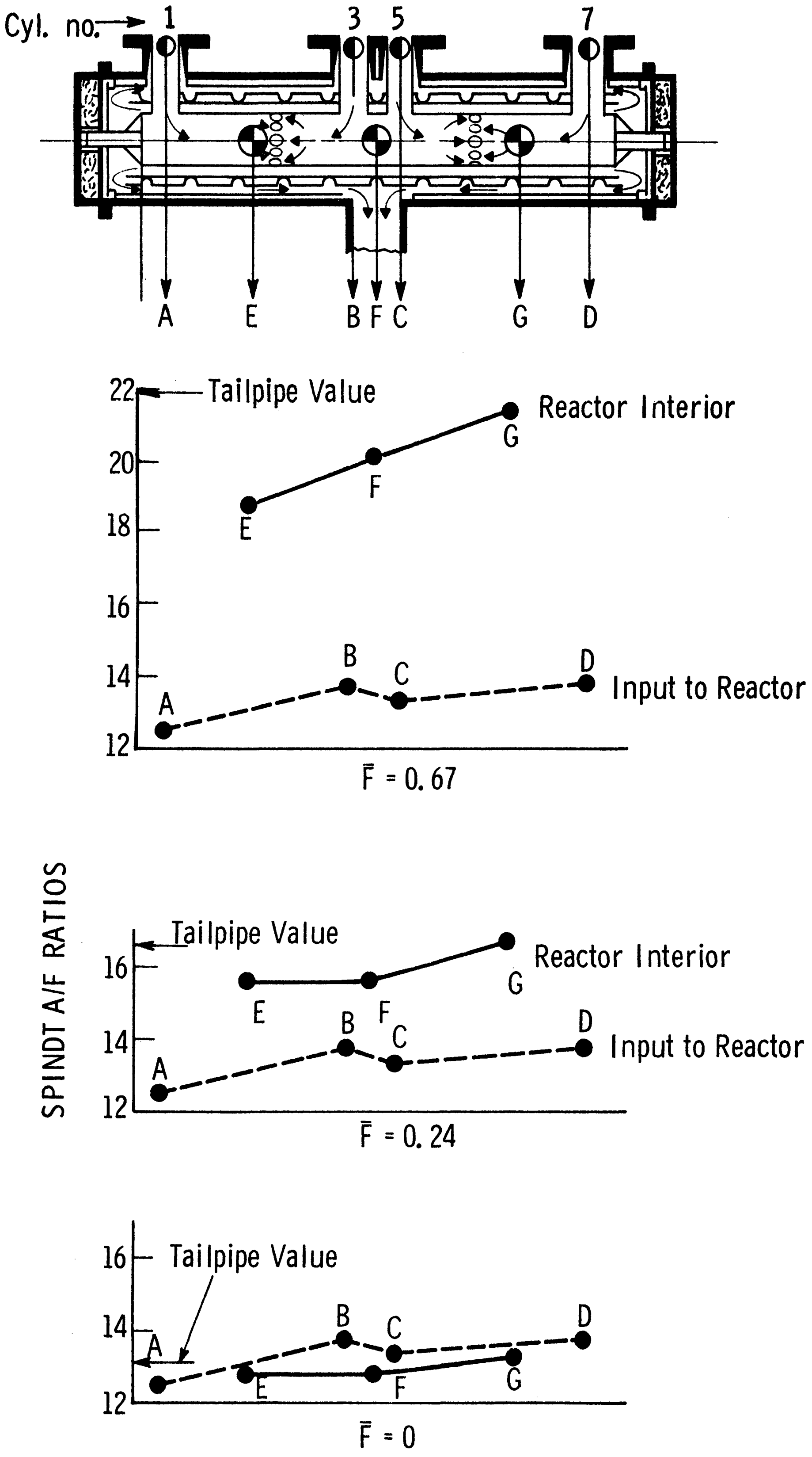

Figure 12. Calculated air-fuel ratio in reactor as a function of air injection fraction $\bar{F}$. Exhaust port values are shown along with average tail pipe air-fuel ratio.

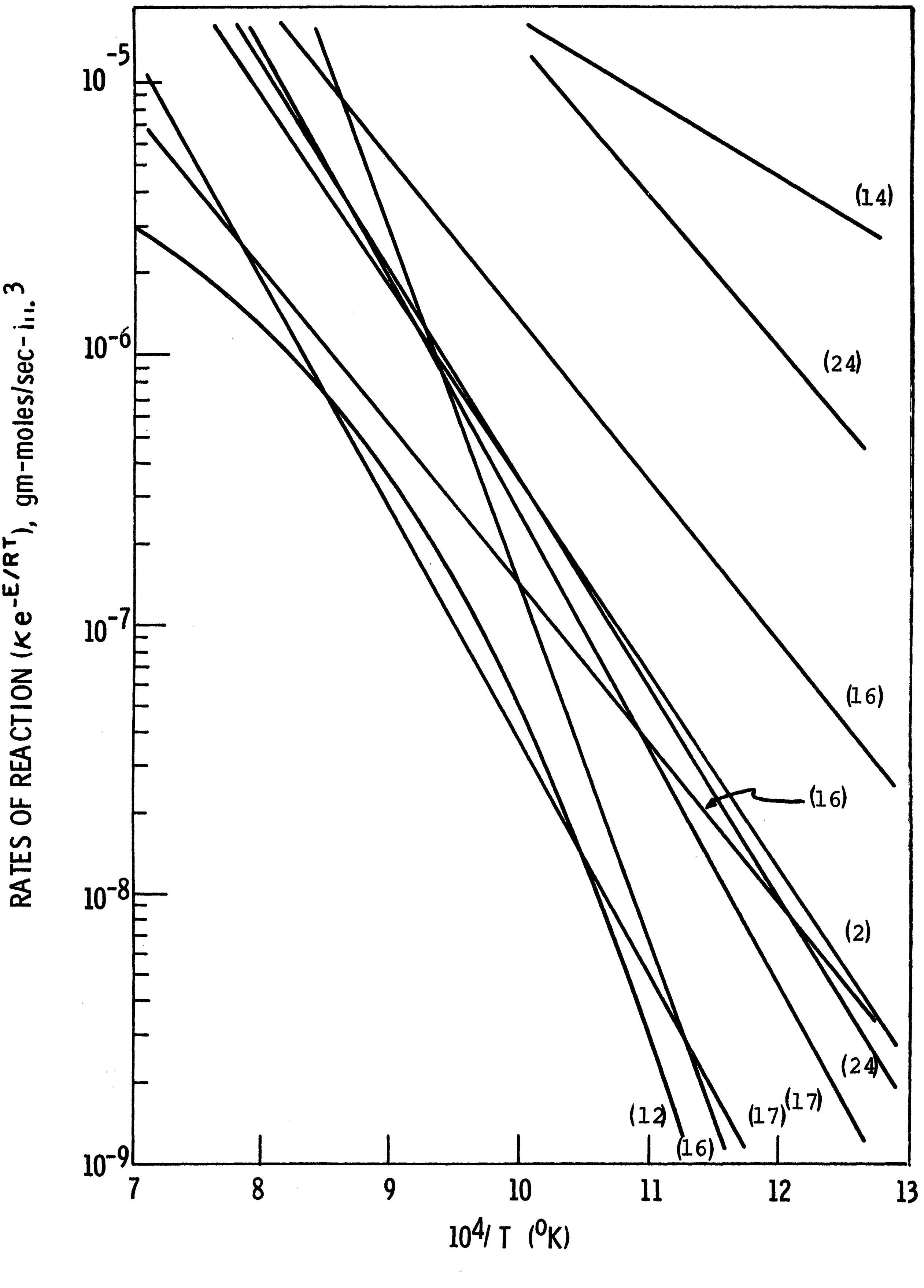

Figure 13. Comparison of reaction rate equations for oxidation of carbon monoxide.

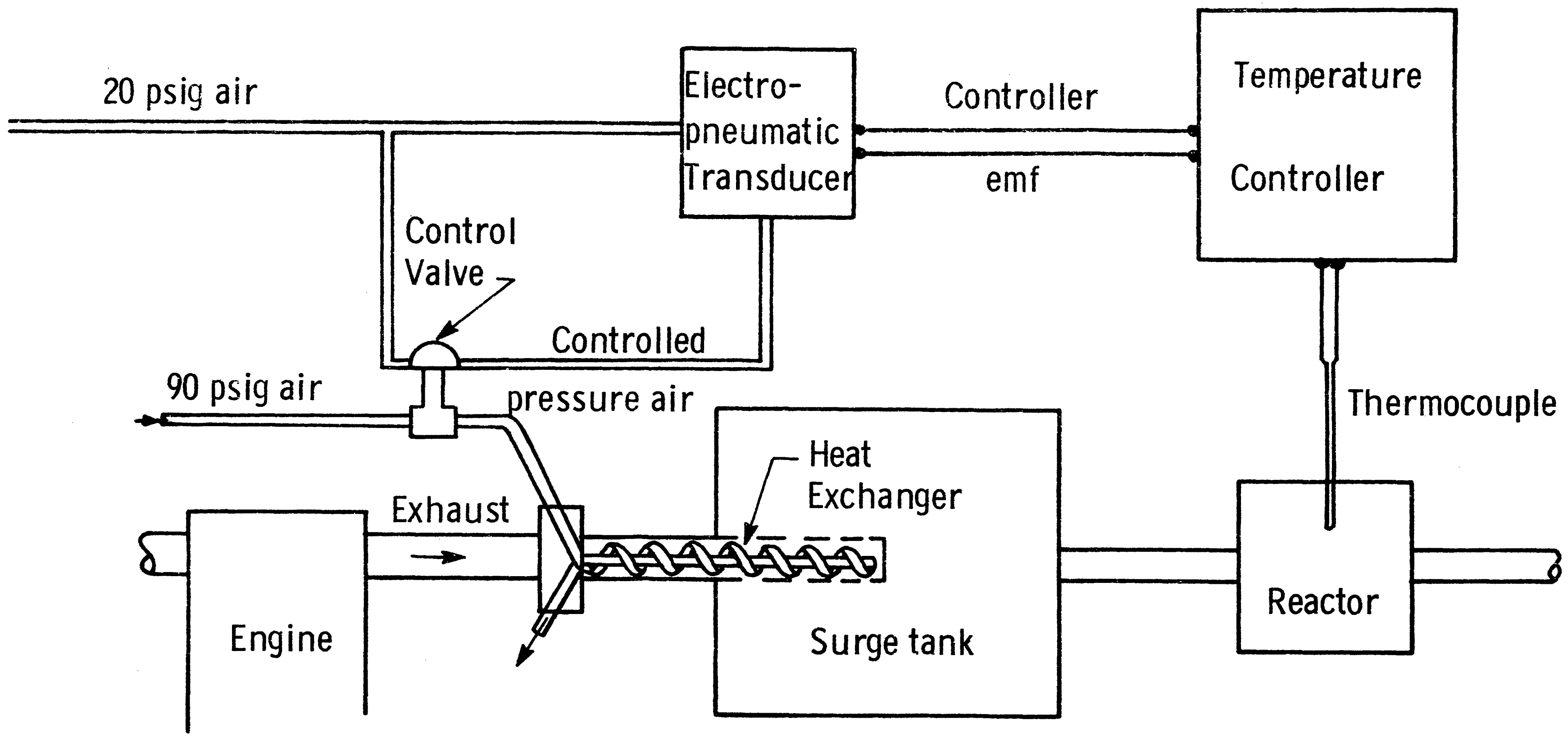

Figure 14. Schematic of test reactor system, with controls.

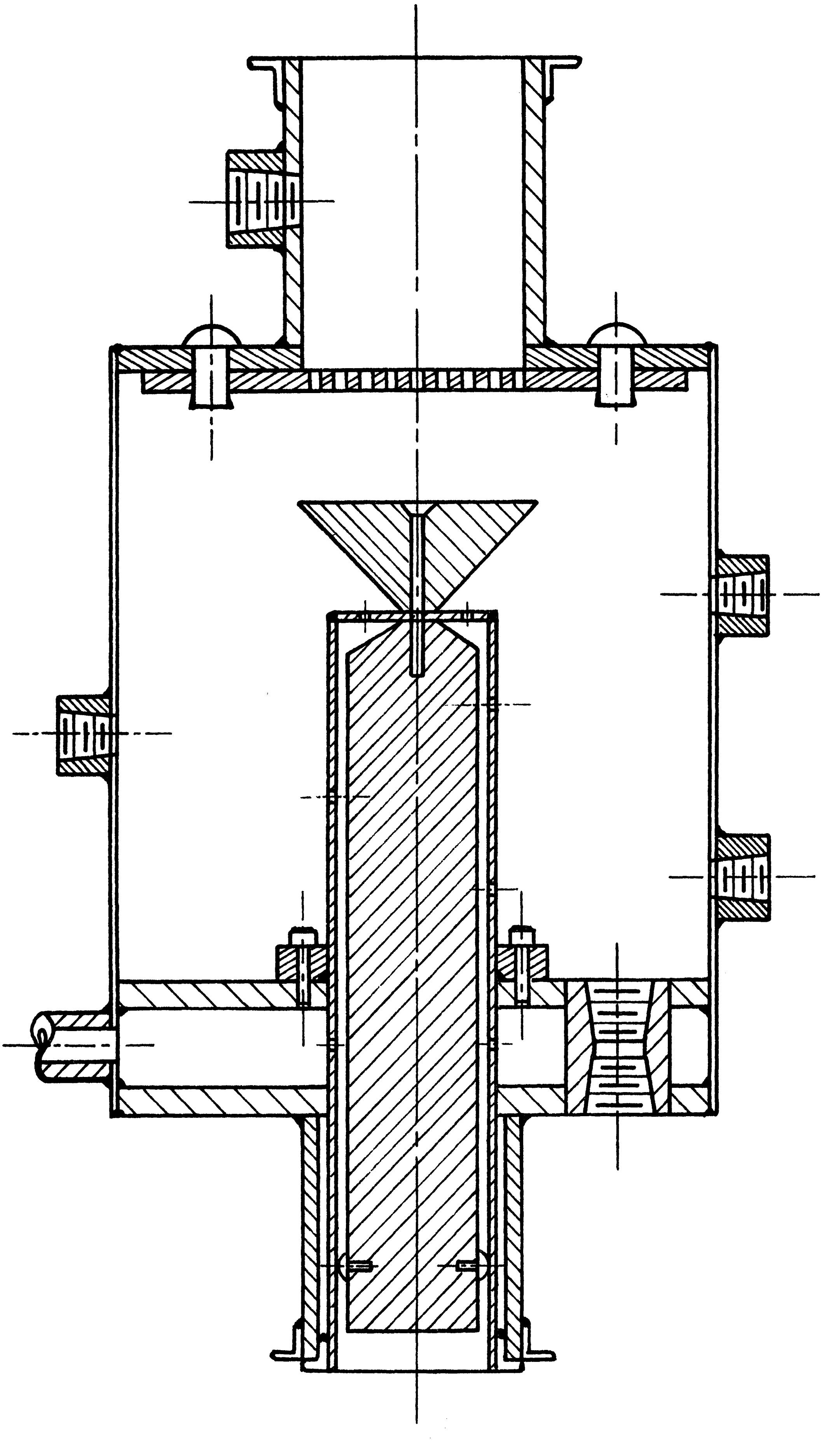

Figure 15. Experimental reactor in modified form.

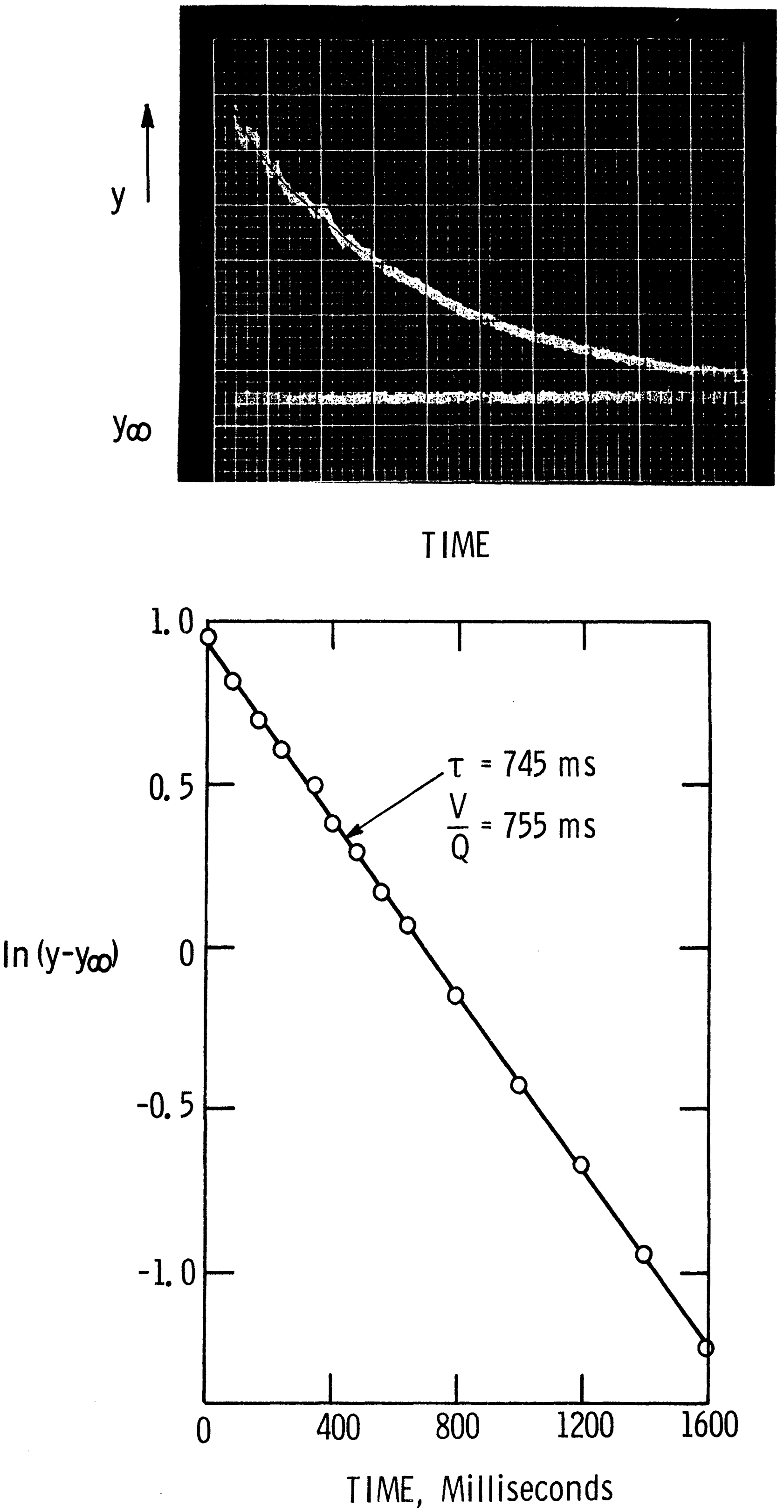

(e) $\dot{m}_{eq}$ = 27lbm/hr

Figure 16. Residence time trace from helium step-change experiment.

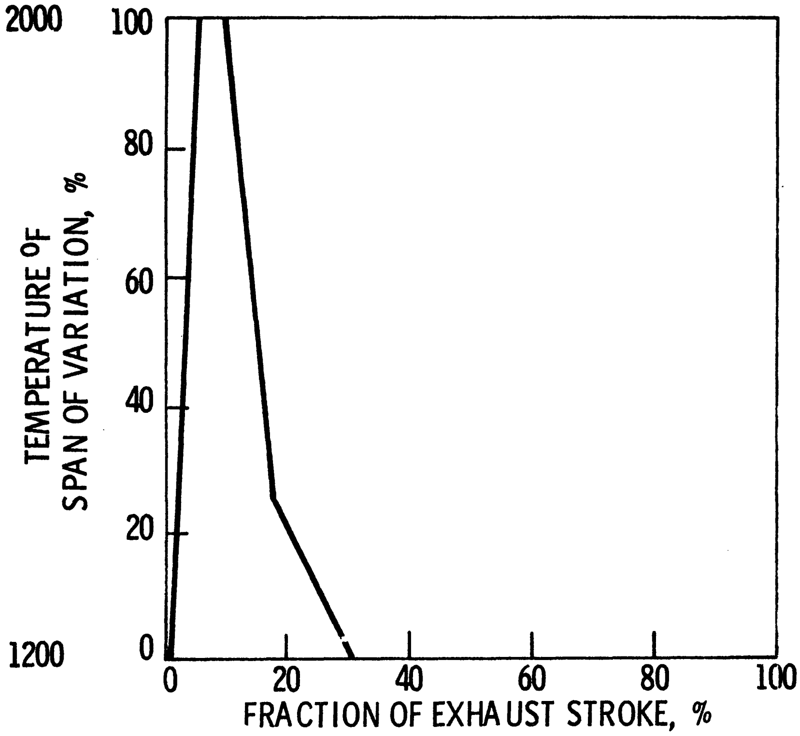

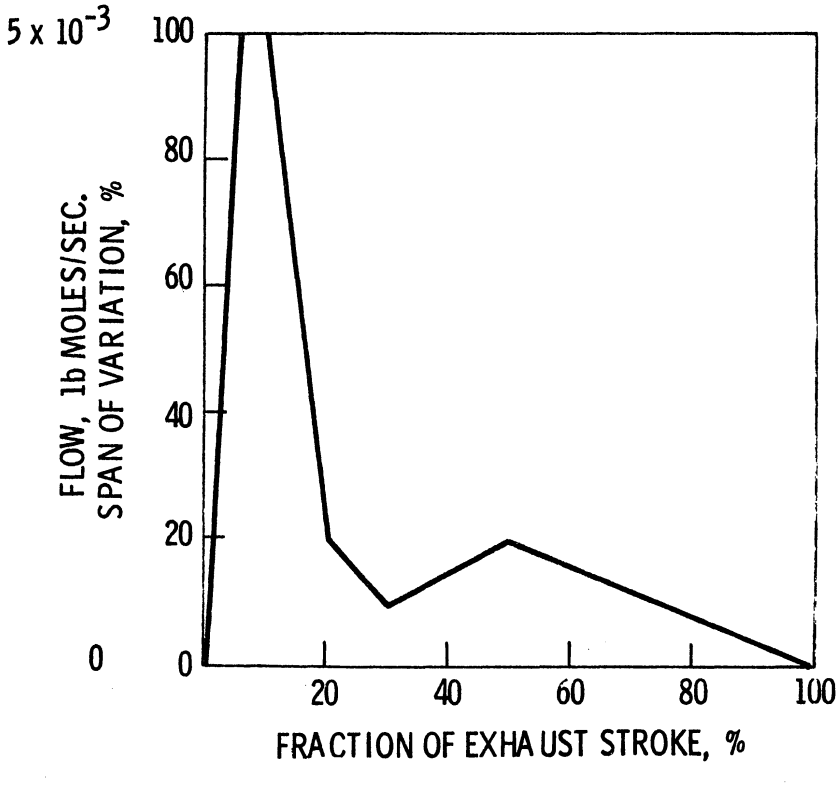

Figure 17. Hypothetical input temperature and flow variations used in preliminary simulation.

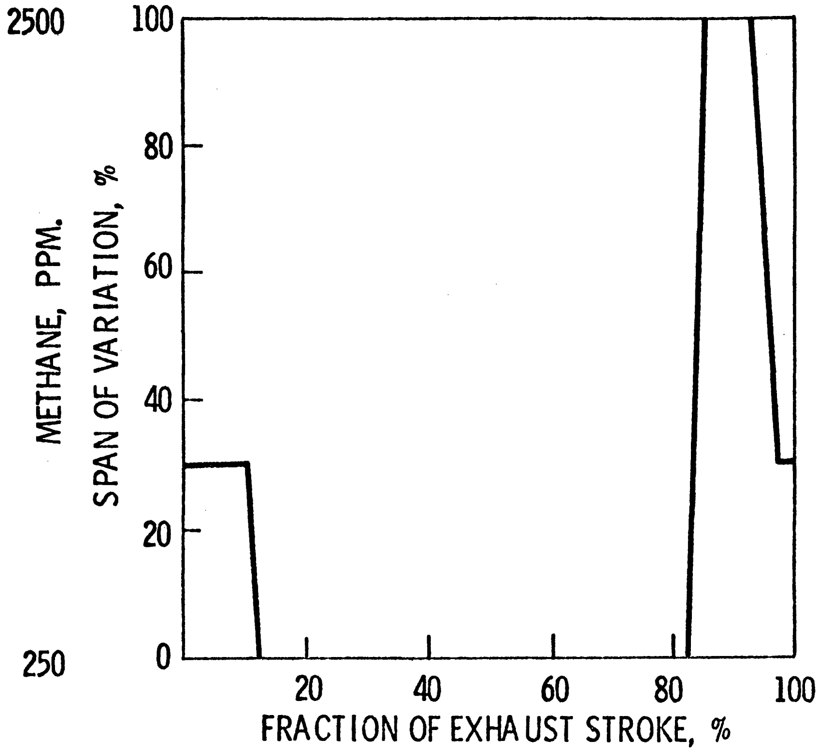

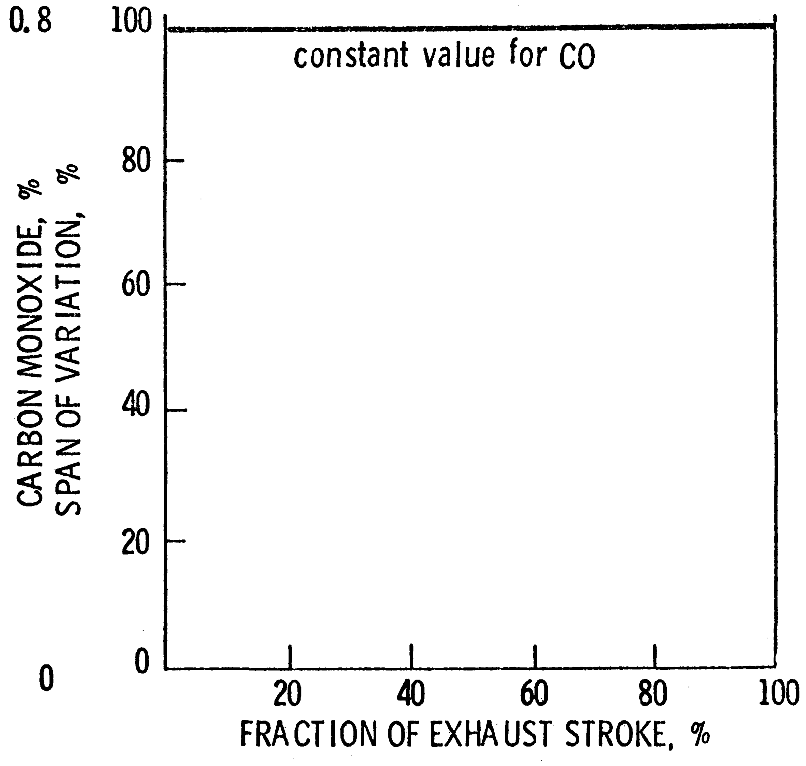

Figure 18. Hypothetical hydrocarbon and carbon monoxide variations used in preliminary simulation.

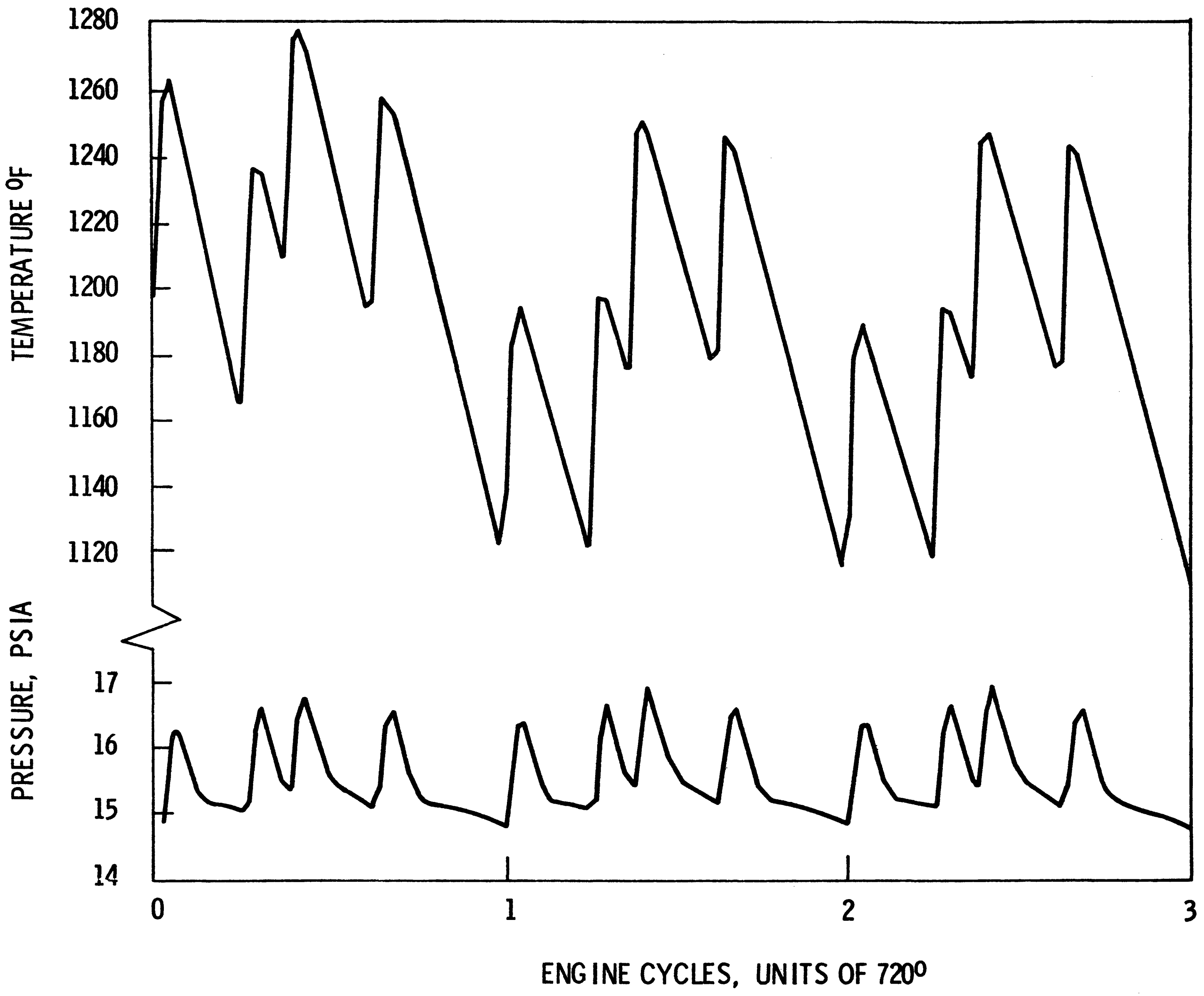

Figure 19. Temperature and pressure in reactor, preliminary simulation.

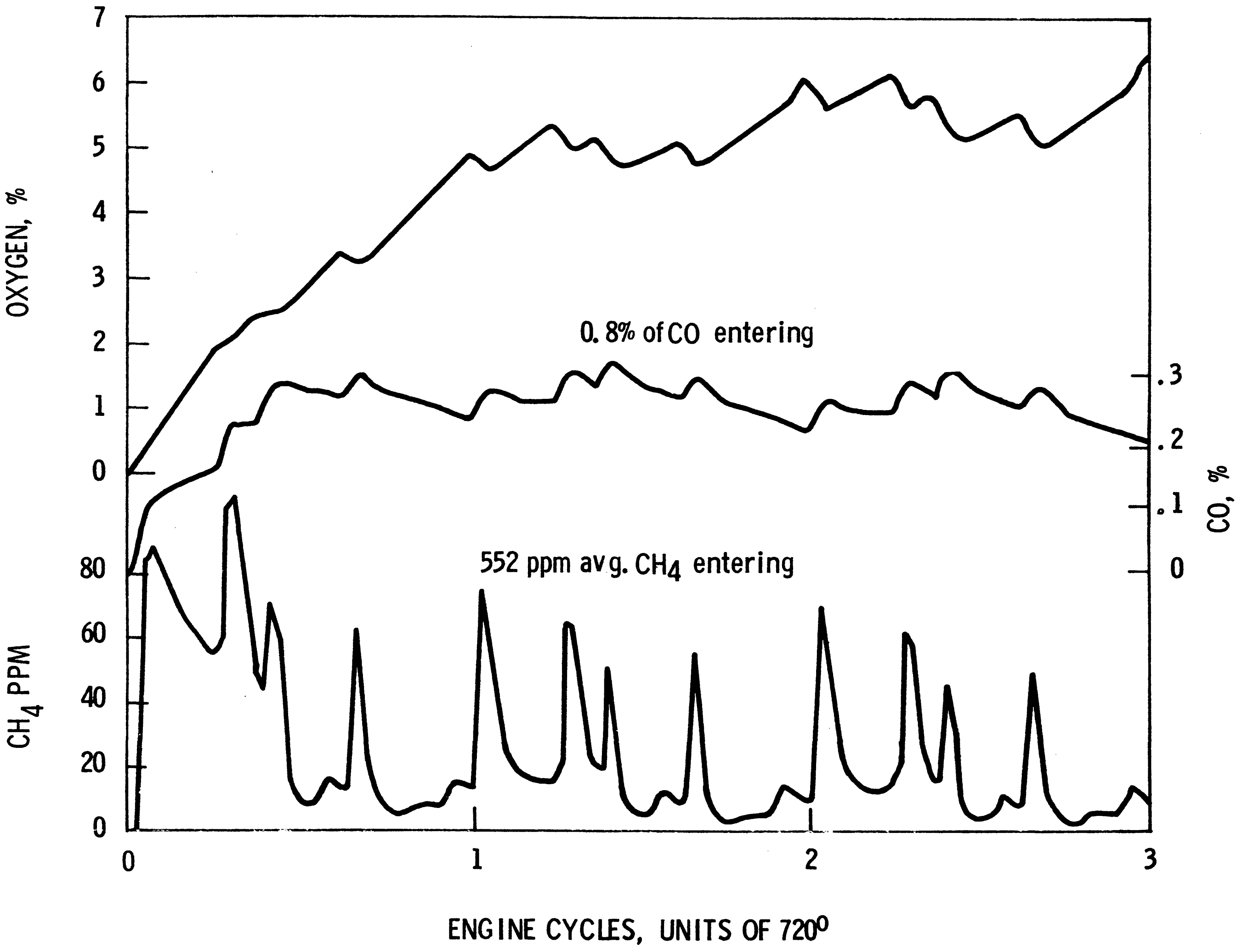

Figure 20. Emission concentrations in reactor, preliminary simulation.